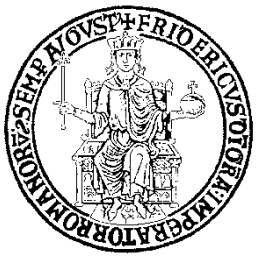

DOCTORAL THESIS

Presented to the Department of Pharmacy
PhD Course: "Scienza del Farmaco – XXXIV Cycle

University of Naples Federico II

Ph.D. Thesis

TERESA SILVESTRI

Biodegradable microparticles for the treatment of posterior eye segment diseases

Approved by
Ph.D. Supervisor: Prof. Marco Biondi
Ph.D. Program Coordinator: Prof.ssa Maria Valeria D'Auria

A.A. 2018-2021

Index

List of abbreviations

AMD: Age-related Macular Degeneration

ARPE: Human Retinal Pigment Epithelial Cell line

ARVO: Association for Research in Vision and Ophthalmology

BSA: Bovine Serum Albumin

CISPL: Cisplatin

CIT: Citicoline

CTRL: Control

DAPI: 4',6-diamidino-2- phenylindole

DME: Diabetic Macular Edema

DSC: Differential Scanning Calorimetry

DR: Diabetic Retinopathy

EMA: European Medicines Agency

ECM: Extracellular matrix

EE: Entrapment efficiency

FACS: Fluorescence Activated Cell Sorting

FDA: Food and Drug Administration

GCL: Ganglion Cell Layer

GDNF: Glial cell-Derived Neurotrophic Factor

GlcA: D-glucuronic acid

GlcNAc: N-acetyl-D-glucosamine

GPC: Gel Permeation Chromatography

HA: Hyaluronic acid

HPMC: Hydroxypropyl Methyl Cellulose

INL: Inner nuclear layer

IVT: Intravitreal injection

MPs: Microparticles

MP empty: Microparticles empty

MP CIT: Microparticles Citicoline

MP PEA: Microparticles Palmitoylethanolamide

MP GDNF: Microparticles GDNF

MTT: 3-(4,5-dimethylthiazol-2-yl)-2,5-diphenyltetrazolium bromide

NMDA: N-methyl-D-aspartic acid

O.C.T: Optimal Cutting Temperature

ONL: Outer nuclear layer

PEA: Palmitoylethanolamide

PGA: Poly(glycolic) acid

PLA: Poly(lactic) acid

PLGA: Polylactic-co-glycolic acid

PLGA MPs: Polylactic-co-glycolic acid Microparticles

PVA: Polyvinyl alcohol

RGCs: Retinal Ganglion Cells

Rhod: Rhodamine

RPE: Retinal Pigmented Epithelium

SVB: Simulated vitreous body

TUDCA: Tauroursodeoxycholic acid

Chapter 1

INTRODUCTION

Chapter 1

1. Introduction

The present research activity concerns the design and development of biodegradable microparticles (MPs), intended as controlled drug delivery systems for the treatment of posterior eye segment diseases. These pathologies, including uveitis, diabetic retinopathy, endophthalmitis, proliferative retinopathy, age related macular degeneration and glaucoma just to cite a few, are generally chronic and degenerative [1], leading in some cases to blindness [2] [3]. These diseases can be treated basically through four routes of administration: topical, systemic, intraocular, and periocular [4]. The topical, systemic and periocular routes do not allow to obtain therapeutically effective drug concentrations in the action site, due to the different biological barriers (e.g., water-blood barrier and blood-retinal barrier, tear dilution, conjunctive/choroidal blood flow and lymphatic clearance), which entail the need of high doses to achieve therapeutic drug levels in the eye [5] [6].

Thus, despite its invasiveness, the intravitreal (IVT) injection is the preferred route of administration to date because it allows the delivery of the therapeutic agents by the target site and the chance to achieve a more effective control of drug concentration within the intravitreal space [7] [5] [8]. Nevertheless, some chronic conditions affecting the posterior chamber of the eye require repeated and frequent injections which cause serious complications such as retinal detachment, cataracts, hemorrhages and endophthalmitis, with an increasing risk of occurrence with increasing number of injections [9] [10] [11]. In this scenario, research activity has been oriented towards the development of several systems for controlled drug release system based on biodegradable polymers such as gels, nanoparticles and microparticles (MPs) [12][13]. The latter, when introduced in the vitreous humor or in the periocular space, generally allow a sustained release of the encapsulated drug(s) [14].

Here, biodegradable microspheres based on PLGA (polylactic-co-glycolic acid) for prolonged intraocular drug delivery have been designed and developed. The main hypothesis is that long-acting

drug delivery systems may help increasing the time interval between two consecutive injections, enhancing patient compliance and reduce the risk of unwanted effect insurgence [15].

It must be highlighted that the intravitreal injection of MPs can cause their free diffusion into the intravitreal space, with a probable blurring of the *visus*. Also, PLGA MPs are intrinsically lipophilic, and therefore they can easily undergo aggregation, with an evident detriment of MP ability to control the release kinetics of the loaded drug(s) [16].

Therefore, MPs were externally decorated with hyaluronic acid (HA), which has been chosen as it is the main constituent of the vitreous body. The central hypothesis of this doctoral thesis is that an increase in affinity between MPs and the vitreous body discourages MP spontaneous diffusion in the eye as well as their aggregation. The MPs were produced with the double emulsion technique and, to physically bind HA to the external surface of the microdevices, the formulation procedure required the use of poloxamers as a physical bridge between lipophilic PLGA and hydrophilic HA.

In a pilot phase of the work, with the intention of defining the optimized formulation, MPs were produced under different formulation conditions and loaded with BSA as a model protein.

In the view of a possible translation of the production method to the industrial reality, different organic solvents to meet the regulatory requirements for human use of the MPs were evaluated. Additionally, the use of different cryoprotectants (namely trehalose, glucose, sucrose and mannitol), was investigated in the perspective of improving the re-suspension of MPs in water immediately before injection.

Lastly, *in vitro* and *in vivo* biological characterization was performed with the focus on glaucoma. For this purpose, the selected formulation was loaded with palmitoylethanolamide (PEA), Citicoline (CIT) and Glial cell-derived neurotrophic factor (GDNF). These molecules were chosen for their expected neuroprotective effect on injured retina [17] [18] [19] [20] and tested *in vitro* on Human

Retinal Pigment Epithelial Cell line (ARPE-19), and *in vivo* on a glaucoma animal model to assess MP safety of use and therapeutic effect.

Chapter 2

STATE OF THE ART

2. State of the art

2.1 Anatomy of the eye

Eye is a sense organ of human body which is responsible for vision. Being unique in its purpose, it has distinctive features such as its specified anatomy and physiology. Eye can be anatomically divided into anterior and posterior segment, which represent one third and two thirds of ocular architecture, respectively. The anterior segment consists of tear, cornea, conjunctiva, anterior and posterior chamber, iris, ciliary body, lens, and aqueous humor, while the posterior segment is composed of sclera, choroid, retina, Bruch's membrane, vitreous humor, optic nerve, and retinal blood vessels.

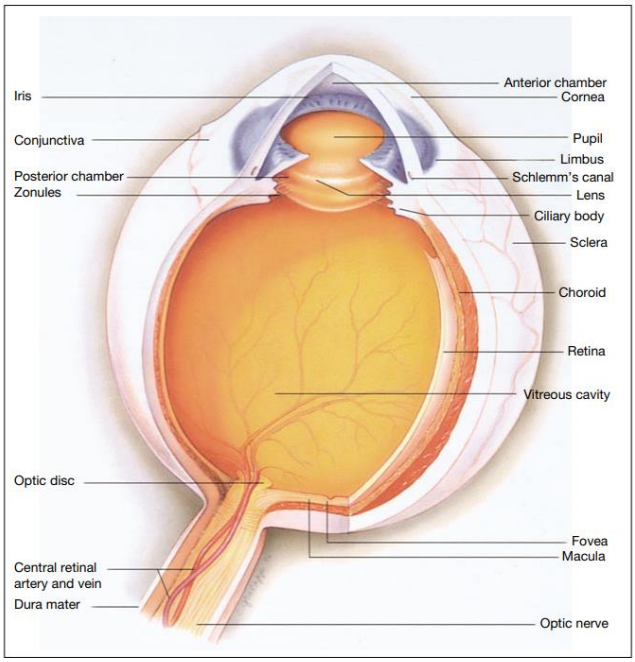

Figure 1: Anatomy of the eye.

Posterior segment eye diseases are defined as the disorders that affect these tissues with the common main outcome of visual impairment and irreversible blindness [6]. The four major causes of severe vision loss in older adults are age-related macular degeneration (AMD), ocular complications of diabetes mellitus, glaucoma, and age-related cataracts [21].

In particular, glaucoma is a progressive neurodegenerative disease that frequently results in irreversible blindness. Indeed, glaucoma causes the death of retinal ganglion cells (RGCs) and their axons in the optic nerve, thereby resulting in deficits of the visual field and, eventually, vision. [22]. Actually, glaucoma encloses a heterogeneous group of ophthalmic conditions that cause the progressive damage to the optic nerve, the primary open-angle glaucoma and the primary angle-closure glaucoma being the most common forms. Most patients with glaucoma suffer from ocular hypertension, but it must be specified that optic nerve damage can occur also with normal intraocular pressure [23]. The treatment of this disease, on the one hand, is aimed to lower intraocular pressure by topical administration of cholinergic agonists, α and β-Adrenergic antagonists, prostaglandins and carbonic anhydrase inhibitors [22]. On the other side, a therapeutic strategy relies upon the neuroprotection of RGCs. Actually, the optic neuropathy of glaucoma involves the axonal injury to the RGC, the cell that projects its axons to the target areas within the brain and carries information for visual function. Thus, the rationale of this therapeutic approach is based on maintaining the state of health of the RGC despite the injury at the optic nerve head to its axon, in such a way as to preserve the structure and visual function [24].

2.2 Intravitreal injection

Pathologies which affect the posterior eye segment are among the major causes of vision loss in developed countries and they are gaining more and more attention due to the increasing life expectancy. These diseases are generally related to the elderly and are mostly chronic and degenerative. For these reasons, these pathologies require frequent and repeated administration of the active molecule to the target site, that is the posterior segment of the eye [2,12].

The intravitreal injection is still the most employed route of administration, since in this case the active molecule is directly inserted into the vitreous body, and this allows overcoming the numerous

biological barriers which hamper the reaching of therapeutic drug concentrations within the posterior chamber of the eye. On the one hand, the intravitreal route is intrinsically associated to serious side effects, such as cataracts, retinal detachment, endophthalmitis and haemorrhages. On the other hand, the injection in the intravitreal cavity ensures a tight control of drug levels within the therapeutic window, which in turn is associated to a reduction of systemic side effects [1, 15]. The first idea of intravitreal injection dates back to 1944 [25], but initially it was not widely employed because of the lack of toxicity studies regarding drugs administered through this route. Currently, the treatment of some acute and chronic pathologies to posterior eye segment involves the repeated intravitreal injection to ensure effective drug levels into the vitreous. However, the low bioavailability of most drugs within the posterior eye chamber, along with the serious drawback related to the intravitreal injection led the research activity, in recent years, to develop drug delivery systems to sustain the release of the active molecules within the eye [21].

Once intravitreally injected, molecules undergo pharmacokinetics issues [26]. Indeed, after diffusion in the vitreous body, the drugs are eliminated *via* anterior and posterior routes. In detail, posterior clearance results into the rapid elimination of the molecule(s) from the vitreous body (half-lives in the order of magnitude of hours), while the anterior clearance is slower and is associated to half-lives in the order of days [27]. Posteriorly, drugs can permeate across the blood ocular barriers in the retina (such as retinal pigment epithelium, RPE and endothelia of retinal capillaries) and the iris–ciliary body. These barriers have intercellular tight junctions that limit the permeation of high molecular weight molecules, whereas small and lipophilic compounds can trespass such barriers up to 50 times faster compared to high molecular weight molecules [28]. Anterior elimination involves drug diffusion from the vitreous to the aqueous humor, and the importance of this route is limited by the iris–ciliary body and the lens. Drugs are eliminated from the aqueous humor through the outflow into the trabecular meshwork. In addition, small molecules can be eliminated from the aqueous humor through the blood flow of the iris–ciliary body. Retinal penetration of nanoparticles and large

molecules can be limited by the inner limiting membrane (ILM). Anti-VEGF molecules are injected every 1–2 months and their intravitreal half-lives is around one week. Due to their high molecular weight, these molecules poorly permeate the blood–retinal barrier and, therefore, most of the dose is eliminated *via* the anterior route [61]. Small-molecule drugs, which are capable of permeating across the blood–retinal barrier, have half-lives of 2–10 hours in the vitreous space, and this requires frequent intravitreal injections, unless slow drug dissolution (e.g., triamcinolone acetonide suspension) or release (e.g., PLGA-based Ozurdex implant for the release of dexamethasone) are obtained [60]. Retinal diseases require chronic treatments, and the dosing interval is an important issue. Therefore, effective, less invasive, and long-acting drug administration strategies are needed.

2.3 Drug delivery systems for posterior eye segment diseases

Drug delivery systems for the treatment of posterior eye segment diseases can be classified into three major categories: intraocular controlled release by implants, drug targeting trough a systemic administration and enhancement of drug permeation trough a barrier, such as the epithelium, endothelium, connective tissue and cell membrane [29].

Innovative intraocular drug delivery systems have been developed in different size ranges aiming to provide therapeutically effective concentrations of the chosen drug(s) for prolonged times within the target site. In particular, these delivery systems are constituted by a combination of drugs and biomaterials, which can be both biodegradable and non-biodegradable depending on the intended region of administration. Based on the size, the devices are roughly classified as implants (> 1 mm), microparticles (1-1000 μm) and nanoparticles (1-1000 nm). According to their physical structure they are divided into reservoir and matrix systems [30]. Implants and microparticles can release the active substance for longer periods of time compared to nanoparticles. More in detail, depending on their physical structure, *reservoir* microparticles are named microcapsules, while *matrix* systems are

named microspheres [29]. Specifically, microcapsules are composed of a core that contains the drug surrounded by a layer made up of a polymer or a mixture of several polymers, while in microspheres the active substance is dispersed in the polymeric matrix. The latter is preferred for biodegradable systems as the drug is dispersed in the polymer.

In case of chronic posterior segment diseases, biodegradable microspheres are most prosing candidates. Indeed, the local administration of biodegradable microspheres offers an excellent alternative to multiple administrations, thus reducing the related side effect of intravitreal injection and enhancing patient compliance.

Furthermore, since most of the retinal diseases are multifactorial, microspheres are remarkably promising because they can be loaded with more than one active substance and complemented with the inclusion of additives with pharmacological properties. Furthermore, a personalized therapy can be achieved with a relative ease by modulating the amount of administered microspheres.

Table 1: Commercial implants as drug delivery strategy for posterior eye diseases.

Product name	Drug	Indication	Sustained release (time)	Materials
Vitrasert® [31]	Gangiclovir	CMV retinitis associated with acquired immunodeficiency syndrome (AIDS)	3 months	PVA, ethylene vinyl acetate
Retisert® [32]	Flucinolone acetonide	Uveitis	30 months	PVA-silicone laminate
Iluvien® [33]	Flucinolone acetonide	DME	18-36 months	Silicone, PVA
Ozurdex® [34]	Dexamethasone	DME, posterior uveitis	6 months	PLGA
Sorudex® [35] [36]	Dexamethasone	Inflammation caused by post cataract surgery	6 months	PLGA, HPMC

2.4 PLGA based microparticles for intravitreal injection

Over the last few decades, the use of biodegradable microparticles as injectable devices has been acquiring an increasing consideration. The erodible devices have a main advantage compared to non-erodible systems since, once degraded, they can progressively leave the site of implantation [37].

Biodegradable polymers such as gelatin, albumin, polyanhydrides and polyesters are the most widely used to produce MPs aimed for intraocular drug delivery. Among them, the derivatives of poly(lactic) acid (PLA), poly(glycolic) acid (PGA) and their copolymers poly(lactic-co-glycolic) acid (PLGA) play a pivotal role. Indeed, the U.S. Food and Drug Administration (FDA) and the European Medicines Agency (EMA) have approved these biopolymers for clinical use, also for ophthalmic purposes and for the treatment of posterior eye segment diseases [38].

Specifically, the equimolar copolymer of glycolic acid and lactic acid (50:50 lactide:glycolide molar ratio) is widely preferred, since it degrades relatively fast to its constitutive monomers, i.e. lactic acid and glycolic acid, which are rapidly eliminated by the body by the Kreb's cycle in water and carbon dioxide [39]. Importantly, PLGA has been approved by FDA for both human and animal use, and this has strongly prompted its widespread application in the clinics for many application [40] [41].

Polylactic acid (PLA) is a biodegradable linear polyester produced from lactic acid. Due to the presence of the chiral carbon center α there are two isomeric forms D- and L-, as reported in Figure 2.

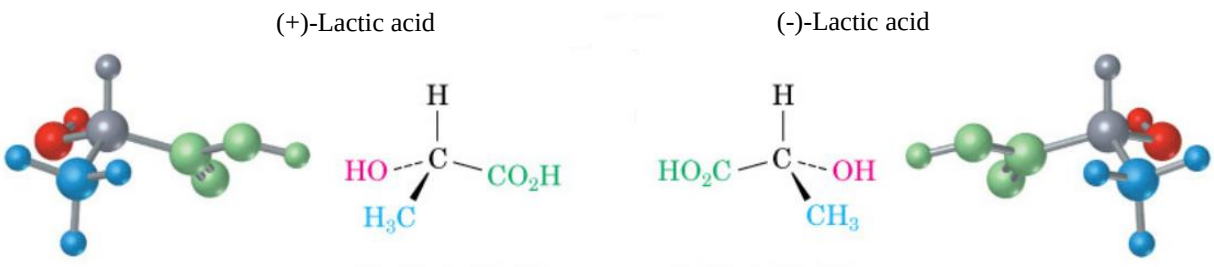

Figure 2. Isomeric structures of PLA.

Poly(L-lactic) acid (PLLA) is biocompatible and biodegradable. Poly(D,L-lactic) acid (PDLLA) has a random distribution of the D- and L isomers along the chain and it is an amorphous and transparent material; its glass transition point is around 57°C (Table 2). Due to its amorphous structure, the degradation kinetics of PDLLA is faster than that of PLLA. Depending on the size and thickness of the sample, the hydrolysis of PDLLA is completed in 2-12 months [42].

Polyglycol acid (PGA), on the other hand, is a highly crystalline solid with 35-75% mass percentage of the crystalline regions, a glass transition occurring between 35 and 40 ºC and a melting temperature is 225-230 ºC; it is also thermally stable, and the time of degradation is 6-12 months (Table 3).

PGA is slowly hydrolysed and degrades in a physiological environment until it is absorbed in about 4 weeks and eliminated in 4-6 months [43] (Table 3).

Table 2. Characteristics and structural formula of PGA, PDLA and PDLLA.

Polymer	*Glass Transition Temperature (°C)*	*Melinting Point (°C)*	*Crystallinity*
Poly(glycolic acid) 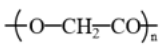	36	230	Higly crystalline
Poly-(D-lactic acid) 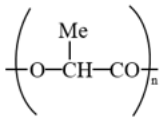	67	180	Higly crystalline
Poly-(D,L-lactic acid) 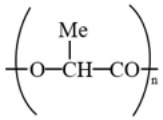	57		Amorphous glass

Table 3. Comparison of different characteristics of PGA, PLA and PLGA.

Polymer type	*Melting point (°C)*	*Glass transition temperature (°C)*	*Degradation time (months)*	*Density (g/cm^3)*	*Tensile strength (MPa)*	*Elongation %*	*Modulus (GPa)*
PLGA	Amorphous	45-55	Adjustable	1.27	41.4-55.2	3-10	1.4-2.8
DL-PLA	Amorphous	55-60	12-16	1.25	27.6-41.4	3-10	1.4-2.8
L-PLA	173-178	60-65	> 24	1.24	55.2-82.7	5-10	2.8-4.2
PGA	225-230	35-40	6-12	1.53	> 68.9	15-20	> 6.9

PLGA (Figure 3) is the copolymer of lactic and glycolic acid and its physico-chemical features change with the molar ratio between the constituting monomer.

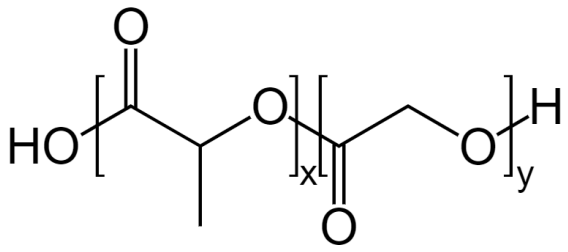

Figure 3: Structure formula of PLGA.

When the molar percentage of glycolic acid is 30-70%, PLGA is generally amorphous and, in particular, the equimolar form has the highest rate of degradation. *In vivo*, the half-life of equimolar PLGA is approximately 15 days, while the complete degradation occurs in about 2 months [44].

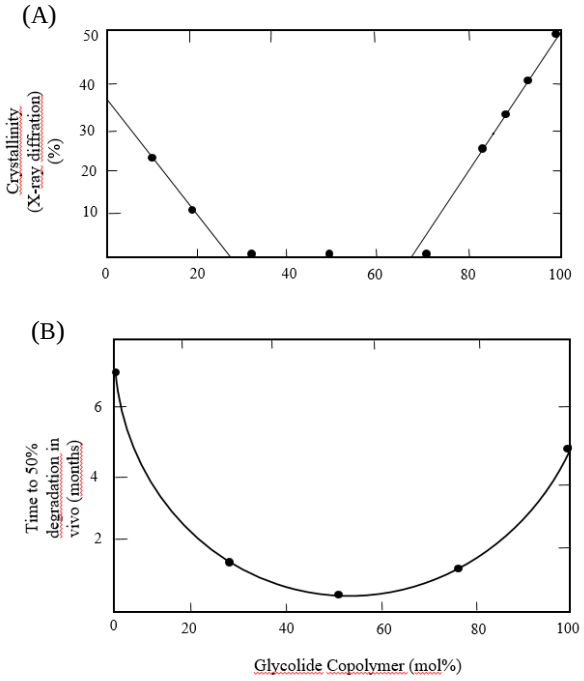

Figure 4. Crystallinity (A) and degradation (B) of PLGA as a function of composition.

For these reasons, PLGA is a material of choice in the production of matrices for the controlled release of drugs [45]. Actually, PLGA polymers are generally preferred to PLA, due to their adjustable mechanical properties and degradation profile. Indeed, different PLGA polymers with tailorable degradation profiles can be synthesised by simply varying the ratio of monomers.

The use of PLGA as a biomaterial to produce drug delivery systems offers a wide range of advantages. For instance, PLGA can be easily solubilised in a wide range of common organic solvents, including chlorinated; moreover, PLGA allows the encapsulation of both hydrophobic and hydrophilic molecules [46]; then, PLGA degradation rate can be purposely modified and predictable. In fact, by properly choosing the molar ratio of the monomers the molecular weight of the polymer, degradation rate and, consequently, drug release kinetics can be tailored with a relative ease. More in detail, an increase of PLGA molecular weight from 10 to 100 kDa causes an increase of the degradation times from several weeks to several months; as for the ratio of glycolic to lactic acid, a higher content of LA correlates with a lower hydrophilicity of PLGA, while equimolar PLGA shows the highest

degradation rate. Moreover, end-group functionalisation also affects PLGA degradation. For instance, endcapping with esters results into polymers with longer degradation half-lives compared to non-endcapped materials displaying free terminal carboxylic acids [47].

In the context of intraocularly administered microparticles, PLGA is a very interesting material for the production of such devices, since it allows to sustain the release of the loaded drugs, therefore holding promise for the reduction of the frequency of administration. This is expected to correlate with a higher patient compliance, and also with the reduction in the potential adverse effects of drug. However, microparticles suffer from some generally common problems such as low loading efficiency, variable burst release and unacceptable organic solvent residuals [48]. Most of these issues can be overcome by the choice/development of proper technologies and methods for microparticle preparation (such as single or multiple emulsion technique or interfacial polymerisation). Anyhow, it must be underlined that the residual solvent content is still a challenge for drug manufacturers.

Table 4. Summary of intraocular PLGA based drug delivery systems.

Carriers	*Materials*	*Drug*	*Diseases*	*Ref.*
Microspheres	PLGA/PLA	Anti-VEGF (Bevacizumab, Ranibizumab), GDNF, Corticosteroids (Dexamethasone), Erythropoietin, Mineralcorticods (Spironolactone), Aciclovir, TUDCA	AMD	[49], [50], [51], [52], [53], [20], [54], [9], [55]
Nanoparticles	PLGA	Anti-VEGF (Bevacizumab, Ranibizumab), Corticosteroids (Dexamethasone), Resveratrol, Fenofibrate,	AMD, DR	[56], [57], [58], [59],
Implants	PLGA	Ganciclovir, Flucinolone acetonide, Dexamethasone	AMD, DR	[10], [11], [12], [13], [14], [15]
Hydrogels	PLGA/ PLGA- PEG-PLGA	Anti-VEGF (Bevacizumab)	AMD, DR	[60], [61], [62]

2.5 Hyaluronic acid decorated MPs for intravitreal release

Hyaluronic acid is a linear polysaccharide constituted of repeated disaccharide units of D-glucuronic acid and N-acetylglucosamine, linked together, alternatively, by β1 → 4 and β1 → 3 glycosidic bonds, as well as by intramolecular hydrogen bonds, which further stabilize the glicosidic bonds conformations. It is ubiquitously present in considerable quantities in the human body in the extracellular matrix (ECM) of connective tissues, in the cartilage, in the aorta, while also being the main constituent of the vitreous body [63]. In addition to its structural function as the backbone of the extracellular matrix, based on its unique physicochemical characteristics and, above all, on its non-toxicity and non-immunogenicity, at least in the most purified forms, HA has found wide application in the biomedical field, especially in eye surgery and osteoarthritis therapy [64].

The idea of external decoration of MPs is a transposition of a previous technique employed to formulate nanoparticles. Indeed, in a previous research activity, PLGA-based nanoparticles were produced by coating with hydrophilic HA for the active targeting of chemotherapeutic drugs by emulsion [65] or nanoprecipitation technique [66]. HA external decoration was physically obtained using amphiphilic poloxamers as 'bridging' molecules between hydrophobic PLGA and hydrophilic HA. In this work, this same formulation technique was translated from the nano- to the micro-scale. For this purpose, HA-coated MPs based on a PLGA/poloxamers organic blend were produced by a slightly modified double emulsion-solvent evaporation technique. The formulation of PLGA-based MPs decorated with HA allows to obtain several advantages. First, by ensuring a controlled release of the drug, a stable active concentration could be provided, thus reducing the number of administrations, and promoting patient compliance. Moreover, the presence of HA molecules on MPs surface is expected to increase the affinity and the interaction with the surrounding vitreous body, which is composed of the same polysaccharide. Indeed, it has been hypothesized that this affinity can act as an obstacle for the aggregation and diffusion of the MPs within the vitreous body, therefore reducing the amount of MPs freely diffusing within the vitreous body. This, in turn, is expected to

decrease the possible interference of the devices floating withing the vitreous space with the visual axis.

2.6 Objectives

In this doctoral activity, HA-decorated, PLGA-based microparticles for the treatment of posterior eye segment diseases, with a special focus on glaucoma, were designed, produced, and tested. The core objective was to obtain sustained release microparticles to reduce the administration frequency in possible clinical application.

The aim of this work is to investigate the capability of the produced microparticles to sustain the release of proteins and drugs and, at the same time, assess how HA can reduce the transport of microspheres within the vitreous body. HA corona was produced in the absence of a chemical reaction, and to this aim the use of poloxamers was necessary to blend the hydrophilic polysaccharide to the lipophilic PLGA.

The developed microparticles are presented as a promising solution to this scope. These devices must face different hurdles, such as the chemical reaction-free design principle which causes complex interactions among the constituent materials and the translation to the biological environment. The main hypothesis is that the surface modification of microparticles can help controlling the site of deposition within the eye.

In a first, part of the work, the effect of HA molecular weight on microparticle transport features in simulated vitreous body was investigated. This part was intended also to evaluate how the poloxamers presence within microparticle matrix affects the release and degradation features of microparticles.

In a development of this part, the impact of varying PLGA:poloxamers ratio on protein release was systematically studied. Indeed, protein release profiles and microparticle degradation kinetics are intertwined and they all directly depend on the composition of the polymeric matrix of microparticles.

A further aim of this activity was to select the most promising formulations in the view of the following parts of the study.

Thereafter, in the perspective of translation from the lab scale to the industrial production, the selected microparticle formulations were loaded with palmitoylethanolamide (PEA), citicoline and glial cell-derived neurotrophic factor (GDNF). These active molecules were chosen for their expected neuroprotective effect on injured retina. Specifically, microparticle preparation method and freeze-drying process were the main focus of this activity.

Finally, the optimized formulations were tested for their biological performance, both *in vitro*, on Human Retinal Pigment Epithelial Cell line (ARPE-19) and *in vivo*, on a glaucoma rat model. The aim was to assess the possible toxicity and efficacy of the produced MPs against the chosen cell populations and living tissues in the eye of the rat.

Chapter 3

MATERIALS AND METHODS

Chapter 3

3. Materials and Methods

3.1 Materials

Poly(D,L-lactide-co-glycolide) (PLGA) (Resomer® RG504H; lactide/glycolide ratio 50:50; inherent viscosity: 0.57 dL · g^{-1} in chloroform at 25 °C) was obtained from Evonik (Essen, Germany). HA with a MW of 180 kDa was kindly offered by Altergon Italia s.r.l (Italy) while HA of 1600 kDa was provided by DSM (Kaiseraugst, Switzerland). Two different poloxamers (PEOa-PPOb-PEOa) were employed: F127 (a = 100 and b = 65, GPC in THF; Mw = 13.8 kDa, Mn = 10.1 kDa; intrinsic viscosity: 0.19 dL · g^{-1} in THF at 35°C) and F68 (a = 76 and b = 29, GPC in THF; Mw = 9.6 kDa, Mn = 8.8 kDa, intrinsic viscosity: 0.15 dL· g^{-1} in THF at 35°C). F68 and F127 poloxamers were provided from Lutrol (Basf, Germany). All other chemicals, i.e., bovine serum albumin (BSA), ethanol (EtOH), acetone, dimethylsulfoxide (DMSO), dichloromethane (DCM), acetone, ethyl acetate, sodium azide, agar, rhodamine, sodium phosphate (Na_2HPO_4), potassium chloride (KCl), sodium chloride (NaCl), GDNF (Glial derived cell neurotrophic factor), ELISA kit, PEA (Palmitoylethanolamide), glucose and sucrose were obtained from Sigma–Aldrich (USA). Citicoline was purchased from ACEF (Italy). Threalose and mannitol were kindly provided by Lisapharma (Erba, Italy). Acetonitrile (ACN) HiPerSolv-CHROMANORM and water HPLC-grade were obtained from VWR (USA). Disodium phosphate dodecahydrate $Na_2HPO_4 \cdot 12H_2O$ and sodium phosphate dihydrate $NaH_2PO_4 \cdot 2H_2O$ were purchased from Farmalabor (Italy).

All the chemical substances were employed without any purification.

3.2 Microparticles production

The first part of the research activity was intended to formulate MPs loaded with BSA, with a theoretical protein loading of 0.2% (0.20 mg of BSA *per* 100 mg of microparticles), externally coated with HA. MPs were fabricated by using a slightly modified double emulsion–solvent evaporation technique. For microparticles production any chemical reaction was avoided, and a lipophilicity gradient between an aqueous phase and an organic phase of the emulsion was exploited. In detail, 0.25 mL of an internal aqueous phase (W_0) consisting of a BSA solution (0.4% w/v) in phosphate buffer (PBS, 1.420 g of Na_2HPO_4, 0.201 g of KCl and 7 g of NaCl in 1 L of purified H_2O) were poured into 2.5 mL of a 20% w/v organic solution (O) of PLGA/F68/F127 (1:0.5:0.5 weight ratio) in dichloromethane (DCM). When necessary, 5 μL of a rhodamine solution in DCM (0.1% w/v) were added to the organic phase to obtain fluorescent particles used in diffusion studies. The two phases were then emulsified by a high-speed homogenizer (Diax 900 equipped with a 10G probe, Heidolph, Germany; 11,000 rpm, 2 min) and the obtained water-in-oil primary emulsion was poured in 40 mL of an external aqueous phase (W_1) and further homogenized at 11,000 rpm (10G probe) for 2 minutes, to obtain the final double emulsion. The external aqueous phase contained 7.5 mg of F68, 7.5 mg of F127 and 30 mg of hyaluronic acid. In the case of control PLGA MPs, the organic phase was a 20% w/v solution of PLGA in DCM, while the external aqueous phase was produced without HA containing only F68 and F127 poloxamers. The organic solvent was then evaporated overnight under magnetic stirring (MR 3001 K, Heidolph, Germany) at room temperature for MP hardening, which were finally centrifuged (5000 rpm, 4°C), washed with distilled water three times (Universal 16R, Hettich Zentrifugen, Germany) and lyophilized for 24 h (-80°C, 0.1 mbar, 24 h; LyoQuest, Telstar, Japan).

The second part of the research activity aimed to optimize the formulation conditions, regarding the polymer concentrations and PLGA/poloxamers ratios, in order to evaluate the influence of poloxamers presence on degradation rate and protein release kinetics. The MPs were produced by the

same double emulsion–solvent evaporation technique previously described in which the organic phase (O), was composed of 20% or 24 % w/v overall polymer concentration and different PLGA/poloxamers weight ratios (50:50, 90:10 or 70:30 w/w) in DCM were employed, as summarized in Table 5. As a control, PLGA MPs were produced with an organic phase composed of PLGA only (20% or 24% w/v), while the external aqueous phase was obtained in the absence of HA.

Table 5. Composition and naming of microparticles.

Formulation name	Overall polymeric concentration %	PLGA:POLOX ratio	PLGA, mg	F68, mg	F127, mg
20-100	20	100:0	500	0	0
20-90	20	90:10	450	25	25
20-70	20	70:30	350	75	75
20-50	20	50:50	250	125	125
24-100	24	100:0	600	0	0
24-90	24	90:10	540	30	30
24-70	24	70:30	420	90	90

Subsequently, in the perspective of the industrial translation of MP production, the preparation method and the freeze-drying process have been taken into account. Specifically, several batches of MPs were prepared employing different organic solvents and cryoprotectants, to overcome many aspects of the regulatory affairs. Indeed, the use of DCM poses some safety and regulatory hurdles, since the residual solvent in the produced MPs has no pharmacological effect but can be rather toxic for both human health and environment. For this reason, to ensure a higher safety level after MPs production, DCM was replaced by acetone, ethyl acetate and DMSO, while keeping the same amount of the aqueous/organic phases.

Once MPs were centrifuged, different cryoprotectants were added in MPs suspension, which are: trehalose, glucose, mannitol and sucrose with the same concentration of 15% w/v with respect to the external aqueous phase. Then, MPs were lyophilized for 24 h (-80°C, 0.1 mbar, 24 h; LyoQuest, Telstar, Japan) and the lyophilized MPs with cryoprotectants were resuspended in purified water and tested for their size distribution (Mastersizer 3000E, Malvern Panalytical, Malvern, UK).

Finally, once the method and formulation conditions were optimized, MPs were loaded with three selected active molecules, reported in the following:

- PEA was solubilized in the organic phase (O) (6.3 mg in 2.5 ml of DCM).
- Citicoline was solubilized in the internal aqueous phase (W_0) (125 mg in 250 µl of BSA solution in PBS).
- GDNF was added in internal aqueous phase (W_0) by dissolving 10 µg in 250 µl of BSA solution in PBS.

3.3 Microparticles Size

MPs were analysed for their mean diameter and size distribution by laser diffraction (Mastersizer 3000E, Malvern Panalytical, Malvern, UK). The tests were run by dispersing MPs in double-distilled water under continuous stirring at 1500 rpm. The mean diameters and the standard deviation were averaged on triplicate samples.

3.4 Microparticles morphology

Scanning electron microscopy (SEM) (Phenom XL, Phenom World, the Netherlands) was employed to analyze MP external shape and morphology after production. The samples were prepared by gold-sputtering under vacuum.

3.5 Microparticles Yield and Protein Entrapment Efficiency

MP yield was gravimetrically obtained from the entire mass of MPs recovered after lyophilization (−80°C, 0.1 mbar, 24 h; LyoQuest, Telstar, Japan), while the actual loading of BSA into the MPs was determined by the Bradford assay. Briefly, for each batch, 10 mg of MPs were solubilized in 500 µL of dichloromethane. Then, 200 µL of PBS (pH = 7.4) were added and the suspension was centrifuged (10000 rpm, 10 min; MIKRO20; Hettich, Tuttlingen, Germany) and 35 µL of the aqueous solution was withdrawn and diluted with 665 µL of the Bradford reagent for 15 min. Afterwards, BSA was quantified by a spectrophotometric assay (UV-1800, Shimadzu; λ = 595 nm), employing a quartz cuvette (6030-UV, d = 10 mm, Hellma Analytics). The linearity of the response was measured in the 0.49–500 µg/mL BSA concentration range ($r^2 > 0.96$). Results are expressed as actual BSA loading (mg of loaded BSA per 100 mg of MPs) and BSA encapsulation efficiency (ratio of actual and theoretical BSA loading rate × 100) ± the standard deviation of the values collected from at least three different batches.

3.6 PEA and Citicoline Entrapment efficiency

- *MP PEA sample preparation:* 1.7 mL of MP suspension loaded with PEA, after centrifugation, were withdrawn and placed in volumetric flask; acetonitrile was added until a final volume of 10 mL was attained.
- *MP Citicoline sample preparation:* 1.25 mL of MP suspension loaded with PEA, after centrifugation, were withdrawn and placed in volumetric flask; acetonitrile was added until a final volume of 10 mL was attained.

Preparation of mobile phase: disodium phosphate dodecahydrate (2.5 g) was dissolved into 700 mL of HPLC-grade water and stirred until dissolution. Then, sodium phosphate dihydrate (0.5 g) was added and, if necessary, the pH of solution was adjusted to pH=7.4; water was added until the final

volume of 1 L. The buffer solution was filtered through 0.2 µm cellulose acetate filter. The conditions employed for HPLC tests are reported in Table 2 and Table 3.

Table 6. Equipment and experimental conditions of MP PEA entrapment efficiency.

HPLC System	Agilent series 1200
UV detector	Agilent series 1200 – G1314B
Column	XTERRA MS -C18 (Waters), 5 µm, 100x2.1 mm
Guard Column	Guard Cartridge for XTERRA MS -C18
Mobile Phase	(**A**) ACN; (**B**) phosphate buffer pH:7.4
Elution mode	Isocratic: 65% (**A**) - 35% (**B**)
Flow rate	0.6 mL/min
Injection volume	4 µL
λ	210 nm
Column Temperature	25°C
Run Time	10 min
Rt PEA	3.9 min

Table 7. Equipment and experimental conditions of MP CITICOLINE entrapment efficiency.

HPLC System	Agilent series 1200
UV detector	Agilent series 1200 - G1314B
Column	SphereClone-C18 (Phenomenex), 3 µm NH2, 150x4.6 mm
Guard Column	Guard Cartridge for SphereClone-C18 3 µm NH2
Mobile Phase	(**A**) ACN; (**B**) sodium phosphate dihydrate solution 10 mM
Elution mode	Isocratic: 10% (**A**) - 90% (**B**)
Flow rate	1 mL/min
Injection volume	10 µL
λ	274 nm
Column Temperature	25°C
Run Time	15 min
Rt CITICOLINE	9.8 min

3.7 GDNF Entrapment Efficiency

5 mg of MP GDNF were dissolved in 0.7 mL of DCM and 0.7 mL of BSA in PBS solution (1% p/v). Then, the samples were vigorously vortexed for 1 minute and centrifuged for 15 minutes (11300 rpm; MKRO). Afterward, the supernatant was removed and 0.7 mL of BSA in PBS (0.1% p/v) were added to the organic phase. The sample was centrifuged with the same previous condition (15 minutes, 11300 rpm) for four times. Finally, the GDNF encapsulation efficiency was determined by ELISA

test, employing a Human GDNF ELISA Kit for serum, plasma, cell culture supernatant and urine (Sigma-Aldrich, USA).

3.8 Preparation of simulated vitreous body (SVB)

Simulated vitreous body (SVB) was prepared following a previously published procedure [67]. Briefly, a solution composed of 0.4 g of Agar and 100 mL of water was led to boiling up until complete Agar dissolution. Subsequently, the hot solution was mixed with 0.5 g of HA (1600 kDa) until a homogeneous mixture was obtained. A few drops of 0.02% w/v sodium azide solution were added to the obtained solution as a preservative and then the solution was cooled to room temperature for 24 hours.

3.9 Rheological properties of SVB

The viscoelastic properties of the prepared SVB were measured by a Kinexus rotational rheometer (Malvern, USA). More in detail, small-amplitude oscillatory shear experiments were performed at 37°C in the 0.1 to 10 Hz oscillation frequency range, and at a strain amplitude at which linear viscoelasticity was attained. The dynamic viscosity was then measured as a function of frequency.

3.10 Transport studies of MPs in SVB

Transport properties of MPs in SVB have been studied through fluorescence measurements. Fluorescent MPs loaded with rhodamine (Rhod) were produced as described in Section 3.2. Only MPs loaded with BSA (MP *empty*) were tested for their diffusion properties. In particular, MPs decorated with 180 and 1600 kDa HA, were the object of this study, using MPs consisting of bare PLGA, *i.e.*, without HA decoration, as a control. Subsequently, they have been evenly incorporated

in the produced SVB (2% w/v) and 200 μL aliquots of this dispersion were placed in the donor chamber of a 1 mL plastic syringe, preliminarily cut in five equal sections (Figure 5). Consequently, the system was composed of one donor section and four receiving sections. Adjacent sections were separated by a nylon web (approximately 0.5 mm average mesh aperture) to enhance an even separation between the sections.

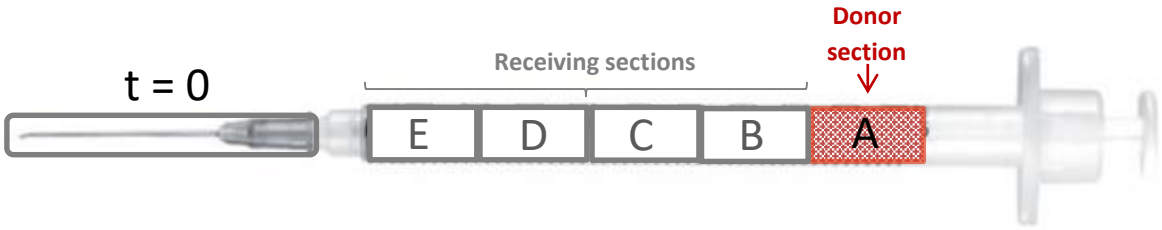

Figure 5. Schematic representation of the diffusion study apparatus.

All the syringes were kept in vertical position, with the tip accurately sealed to avoid SVB loss during the experiments. The top section of each syringe, acting as the donor compartment, contained a 4 mg/ml dispersion of Rhod-loaded MPs in SVB. Then, the syringes were incubated at 37°C and, at scheduled time intervals, were withdrawn, and the single sections separated and immediately frozen at -20°C to anneal further transport. Subsequently, the content of each section was dissolved in 2 mL NaOH 0.5 N and analyzed for Rhod content by spectrofluorimetric analysis at λ = 553 nm (Varian Cary Eclipse Fluorescence Spectrophotometer, Thermofisher, USA), using a quartz cuvette (6030-UV, d = 10 mm, Hellma Analytics, USA). The linearity of the response was assessed in the 0.125 – 2 mg/mL MP concentration range ($r^2 > 0.99$). Fluorescence data were corrected for Rhod release at any time and for each section.

3.11 BSA release kinetics

In vitro release profiles of BSA from PLGA-based MPs were evaluated in SVB. The release kinetics was investigated uniquely for BSA loaded MPs (MP *empty*), decorated with both HA (180 kDa and 1600 kDa), bare PLGA MPs and for MPs whose organic phase presents different poloxamer/PLGA ratio. For each experiment, a dispersion containing 25 mg of MPs in SVB (weight ratio = 1:20) was poured into a vial; then, 1 mL of PBS at pH 7.4 was poured onto the gel and the system was incubated at 37°C in a thermostatic bath. At predetermined time points, 500 µL of supernatant were withdrawn and replaced with fresh PBS, while monitoring the pH of the release medium with litmus paper. BSA was quantified by the Bradford assay and the results are expressed as fraction of BSA released ± the standard deviation of three replicas. The main phenomena dictating protein release were estimated by modeling the released BSA fraction through the equation proposed by Corrigan and Xue, adapted for the MPs produced in this work [68]. In brief, BSA release from PLGA-based MPs was considered to be mainly governed by two major mechanisms, namely solubilization and matrix erosion. The first refers to protein dissolution at the interface between MP porosities/surface and the release medium, which is primarily dictated by protein diffusion through aqueous domains within MP evolving macropores [69]. The second mechanism considers the fraction of released BSA controlled by matrix bulk erosion, which is due to PLGA degradation and poloxamers solubilisation.

The first term is defined by Equation (1):

$$\varphi_S = \varphi_{S,\infty}[1 - exp(-k_S t)] \qquad (1)$$

where φ_S is the fraction of BSA released due to solubilization at time *t* [day]; $\varphi_{S,\infty}$, is BSA fraction released after a virtually infinite time if no other phenomena contribute to BSA release; k_S [day^{-1}] is the solubilization rate constant. Erosion-controlled release refers to $(1 - \varphi_S)$, which is the fraction of the protein entrapped within MPs, which is described by the following Equation (2):

$$\varphi_E = (1 - \varphi_S)\frac{exp[k_E(t-t_{MAX})]}{1+exp[k_E(t-t_{MAX})]} \qquad (2)$$

Here, k_E [day^{-1}] is the erosion constant, which takes into account the loss of matter due to both PLGA autocatalytic degradation and poloxamers dissolution; t_{MAX} [day] is the time at maximum release rate. The sum of Equations (1) and (2) provides the total released BSA fraction. The total released fraction, therefore, is given by the sum of the contributions:

$$\varphi_{TOT} = \varphi_{S,\infty}[1 - exp(-k_S t)] + (1 - \varphi_S)\frac{exp[k_E(t-t_{MAX})]}{1+exp[k_E(t-t_{MAX})]} \qquad (3)$$

Equation (3) has been solved by nonlinear least squares fitting using an in-built 4th-order Runge–Kutta method, with with $\varphi_{S,\infty}$, k_S, k_E and t_{MAX} as adjustable parameters.

3.12 Degradation studies of MPs

The degradation studies were performed firstly to determine the mass loss kinetics of MPs decorated with both HA (180 and 1600 kDa). Then, the evaluation of degradation rate concerned the time variation of the molecular weight (weight-average and number average molecular weight, Mw and Mn respectively) by Gel Permeation Chromatography (GPC) as described in Section 3.14. In both cases, merely MP empty were characterized for their degradation profile.

The samples were prepared in both case by the following procedure: MPs were suspended in PBS (0.1% w/v) and incubated at 37 °C in a thermostatic bath. At scheduled time points (7, 14, 21, 28 days), the samples were centrifuged (5000 rpm, 10 min. 4 °C; Universal 16R, Hettich Zentrifugen, Germany) and the PBS supernatant, containing the solubilized MPs fractions, was withdrawn and replaced with an equal volume of fresh PBS. Then, the samples were lyophilized (−80 °C, 0.1 mbar, 24 h; LyoQuest, Telstar, Japan).

3.13 Mass loss kinetics of MPs

The rate of mass loss of the MP decorated with 180 or 1600 kDa HA, only loaded with BSA and with an organic phase composed of 20% w/v overall polymer concentration (PLGA/poloxamers, 50:50) in the organic phase of the emulsion were performed. The residual weight of the lyophilized samples was gravimetrically obtained, taking into account the mass of the salts, preliminarily determined by lyophilizing PBS solutions used as a control (n = 6). The results were expressed as the mean residual mass percentage ± the standard deviations of at least three replicas. As a control, PLGA MPs were examined.

$$100 \times \left(1 - \frac{MP\ Mass\ t_0}{Residual\ MP\ Mass}\right) .$$

3.14 Gel Permeation Chromatography (GPC)

GPC was performed on MP *empty*, decorated with HA 1600 kDa, whose organic phase is composed of 20 or 24 % overall polymer concentration with different PLGA/poloxamers ratios (70:30 or 90:10). Since only a fraction of MPs are soluble in tetrahydrofuran (THF), as a first step MPs were suspended in THF for 24 h at 40°C to solubilize PLGA and poloxamers. The insoluble fraction, composed of BSA and HA, was removed by filtration (PTFE membranes of 0.22 µm porosity), while the soluble phase was dried in order to estimate the exact mass of soluble polymers. Purified samples were redissolved in THF and analyzed using a GPC Max Viscotek system equipped with a TDA 305 detector (Refractive Index, Low Angle Light Scattering, Right Angle Light Scattering and Viscometer) and UV detector. Column set was composed of a pre-column Phenogel Phenomenex and two columns of 10^3 and 50 $g \cdot mol^{-1}$, respectively. The 50 $g \cdot mol^{-1}$ column was selected to take into account the very-low-molecular-weight fraction (low exclusion limit is 100 Da). PLGA, poloxamers

and all the samples reported in Table 1 were dissolved at 2–4 mg/mL concentration and eluted in HPLC-grade THF (Romil) at 40°C. The injection volume was 100 µL and a flow rate of 0.8 mL/min was employed. The chosen method of analysis was universal calibration with PS standard ranging from 66 kDa to 937 Da. The measurements, performed at 35°C according to the temperatures of columns and detectors, were performed for 35 min in duplicate.

3.15 Thermodynamic Analyses by Differential Scanning Calorimetry (DSC)

To determine how the glass transition of PLGA is affected by the release/degradation time and formulation variable, differential scanning calorimetry studies (DSC; TA Q20) were performed to identify the thermodynamic transitions of MP empty during degradation. In particular, the MPs collected at predetermined incubation times were centrifuged, washed and lyophilized. Then, carefully weighed masses of each MP sample (2–5 mg) were placed in hermetically sealed aluminum capsules and subjected to a double dynamic scan (10–80°C; heating rate: 5°C/min) in nitrogen flow at 50.0 mL/min. Glass transition temperatures were obtained during the second scan as the inflection points of the thermograms. Melting points were obtained as the extrapolated onset points in the DSC endothermic peaks, where present.

3.16 In vitro cell cultures

The optimized and lyophilized MP formulations, loaded with Citicoline, PEA, GDNF,were tested by *in vitro* assay, MTT tests and Cytofluorometric assessment of apoptosis (FACS), as described in the following.

The human Retinal Pigment Epithelial cells, ARPE-19 (ATCC-CRL-2302) were cultured in Dulbecco's Modified Eagle medium F12 medium (DMEM/F-12; Sigma-Aldrich, USA)

supplemented with 10% v/v Fetal Bovine Serum (FBS; Gibco, USA), 100 U/mL penicillin, 100 μg/mL streptomycin (Gibco, USA). The cells were seeded in 75 cm^2 flasks and placed in a humidified atmosphere at 37°C with 5% CO_2 and then passaged once a week using 0.25% Trypsin-EDTA (Gibco, USA). FBS concentration was lowered to 1% to perform experiments.

3.17 MTT assay

The cell viability was determined using the 3-(4,5-dimethylthiazol-2-yl)-2,5-diphenyl tetrazolium bromide (MTT) conversion assay. ARPE-19 cells were plated at 20.000 per well in 96-well plates and were grown to 80% of confluence before carrying out the experiments. After the stimulation with empty and loaded MPs (C3 = 5×10^{-4} mg/mL; C4 = 5×10^{-6} mg/mL; C5 = 5×10^{-8} mg/mL), active molecules alone (PEA, C3 = 2×10^{-4} mg/mL; C5 = 2×10^{-8} mg/mL; Citicoline, C3 = 2×10^{-4} mg/mL; C5 = 2×10^{-8} mg/mL, GDNF, C3 = 5×10^{-4} mg/mL; C4 = 5×10^{-6} mg/mL, C5 = 5×10^{-8} mg/mL) for 24, 48 and 72 hours, the cells were incubated with 20 μL of MTT solution (5 mg/mL, Sigma-Aldrich) for 4 hours at 37°C. Then, the formazan crystals formed were dissolved in 200 μL of dimethyl sulfoxide (DMSO) and incubated for 15 minutes. The absorbance of each well was measured at 570 nm and 750 nm served as reference wavelength, using a microplate reader (Victor, PerkinElmer). Cell viability was expressed as the percentage of living cells with respect to the untreated control.

3.18 Cytofluorometric assessment of apoptosis

For apoptosis determination, after the indicated treatments and time points, cells were harvested and stained for 30 min at 37°C with: (i) 20 nM of 3,3′-dihexiloxalocarbocyanine iodide ($DiOC_6(3)$; Molecular Probes, Life Technologies) for mitochondrial transmembrane potential ($\Delta\Psi m$) quantification; (ii) 1 μg/mL of 4',6-diamidino-2- phenylindole (DAPI, ThermoFisher), a dye that incorporate only into dead cells, used for determination of cell viability. Cytofluorometric

acquisitions were performed on a Miltenyi flow cytometer (MACSQuant® Analyzer 10) gating 6000 events per sample. Data (FITC/VioBlue data) were analyzed using FlowJo.

3.19 In vivo tests

The optimized MP formulations, loaded with PEA, Citicoline and GDNF, were tested by *in vivo* assay to evaluate toxicity and efficacy of the produced MPs against the living tissues in the rat's eye.

Thirty-six male Wistar albin rats (Elevage Janvier, Le Genest Saint-Isle, France; age: 8 weeks) were treated in accordance with the ARVO Statement for the Use of Animals in Ophthalmic and Vision Research. All animal experimental procedures were approved by the local ethics committee European Council Charles Darwin, University Paris Descartes (Paris, France). Animals were fed with a standard laboratory diet and ad libitum tap water in a controlled temperature room at 21-23°C. The cyclic light environment consisted of 12 hours of light per day.

3.20 Animal procedures

The design of the study was divided in two experiments: the first one was aimed to verify the MPs toxicity in vivo; the second one to assess the activity of drug loaded MP *in vivo* performed in acute toxic model (NMDA, N-methyl-D-aspartic acid, Sigma-Aldrich, USA), in order to evaluate the rescue of the retinal ganglion cells. [70]

At time of the experiment, rats were 10-week-old and were anesthetized by intramuscular injection of 100 µL/100 g of a solution containing ketamine (40 mg/mL; Ketamine 1,000®, Virbac, Carros, France) and xylazine (4 mg/mL; Rompun 2%®, Bayer Santé, Puteaux, France). Pupillary dilatation was obtained by instillation of two drops of tropicamide (Mydriaticum 0.5%®, Thea, France). Topical ocular anaesthesia with 1 drop of tetracaine hydrochloride (Tetracaine 1%®, Faure, France) was

performed two minutes before injection. After seven days animals were euthanized by carbon dioxide inhalation and both eyes were immediately enucleated for the subsequent analyses.

For the first experiment, animals were randomized into four groups (n = 16) which received intravitreal injection of empty MPs and three different MP formulations loaded with the active molecules (namely citicoline, palmitoyl ethanol ammine and GDNF), in both eyes. The second step required the animals partitioning in five groups (n = 20). The control one didn't receive any injection. For MP injection procedure, 66% (w/v) suspensions of MP were prepared in Hanks Balanced Salt Solution (HBSS) and briefly vortexed immediately before each injection to ensure homogeneous dispersion of MP in the injected suspension. 5 µL (experiment one) or 6 µL (experiment two: 5 µL of MP suspension and 1 µL of NMDA) of MP suspension were administered in the superior pole of the vitreous body using a 31G needle for insulin (100U). NMDA (Sigma, France) was resuspended in sterile BSS at the concentration of 200 mM. Serial dilutions were done to obtained a final solution at 20 mM, so 1µL injected contained 20 nmol of NMDA.

3.21 Histology

After animal euthanization, all eyes were enucleated with a piece of tissue at the superior pole for the right orientation. One eye enucleated from rat was fixed with 4% v/v paraformaldehyde, 0.5% v/v glutaraldehyde (LADD, Inland Europe, Conflans-sur-Lanterne, France), in PBS for 2 h. The other eye was fixed with 4% v/v paraformaldehyde in PBS for 2 hours. After fixation, samples were washed, dehydrated in a graded alcohol series: 2 hours in 70% alcohol and 2 hours in 95% alcohol. Then, a mix of infiltration medium and 95% alcohol for 2 hours was employed. Finally, the samples were stored in the infiltration solution of the Leica historesin embedding kit overnight at 4°C. Samples were embedded in the embedding medium (Leica) and attached to a block holder after polymerization. Plastic sections (5 µm thick) passing through the optic nerve head were prepared on a microtome (Leica Microsystems, France), stuck on slides, and stained 15 minutes with 1% w/v

toluidine blue solution. Sections were observed with a microscope (Leica Microsystems,) and photographed with a Leica Microsystems camera.

3.22 Retina thickness measurement

Thicknesses of outer nuclear layer (ONL), inner nuclear layer (INL) and photoreceptors segments were measured every 500 µm on the section passing on the centre of optic nerve using ImageJ software. Histological sections measurements were performed across the whole retina, considering the inferior pole to 0 from −4000 µm of optic nerve and superior pole to 0 from 4000 µm of optic nerve. Thickness profiles along the retina were generated by averaging, for each distance, the values obtained for all eyes treated similarly to give a single value *per* group.

3.23 Immunohistochemical analysis

Freshly enucleated eyes were fixed for 2 h with 4% v/v paraformaldehyde in 1× phosphate-buffered saline (PBS, Life Technologies), washed with PBS, infiltrated in gradients sucrose series diluted in PBS (10% w/v, then 20% w/v and finally 30% w/v for 2 hours each). Then, the eyes were further mounted in Tissue-Tek O.C.T. (Siemens Medical, Puteaux, France) and frozen with dry ice. Frozen sagittal sections (10 µm) close to the optic nerve were cut by a microtome (Leica). The sections were washed and permeabilized with 1% v/v Triton X-100 for 30 min. After rinsing with PBS, the cryo-sections were incubated for 1 h at room temperature with different primary antibodies (rabbit anti-glial fibrillary acidic protein, GFAP, 1:200, Dako, Trappes, France and CD11b, 1:100) diluted in a primary antibody solution of 0.1% v/v Triton X-100 in PBS. Negative control sections were incubated without primary antibodies. After washing with PBS, the sections were incubated for 1 hour with secondary antibodies coupled with a fluorochrome (goat anti-rabbit 1:200) and donkey anti-mouse, 1:200 (Thermo Fisher Scientific) in a secondary antibody solution (0.1% v/v Triton X-100 in PBS).

Finally, after the rinsing with PBS, slides were stained for the nuclei with 4′,6-Diamidino-2-Phenyl-Indole (DAPI, 1:5000, Roche) for 5 minutes, washed again, and mounted with gel mount. Fluorescently labelled sections were observed under an epifluorescence microscope (Olympus, Rungis, France) equipped with a CCD camera (Olympus DP72) using identical exposure parameters across samples to be compared.

To evaluate activated macrophages/microglial cells, GFAP and CD11b level intensity were measured on entire ocular cross sections at the optic nerve level. CD11b level intensity was also measured in ciliary bodies.

3.24 Quantification of Retinal Ganglion Cells (RGCs)

The second experiment was carried out to evaluate the activity of drug-loaded MPs toward the rescuing of RGCs in acute toxic model of glaucoma. The stress was induced by the administration of NMDA in the MP suspensions.

From the enucleated eye, the retina was removed and cut in four petals. Superior petals were marked. Each explant was fixed with PAF 4% in PBS 1× for 10 minutes. Then, the following step was the permeabilisation/saturation with 5% FBS and 1% Triton X-100 in PBS, for 1 hour at room temperature. The blocking solution was removed by rinsing twice with 0.1% Triton X-100 in PBS for 5 minutes, and the retinal sections were immediately incubated with the primary antibody Brn3a (1:200) (Santa Cruz Biotechnology, Heidelberg, Germany) in a primary antibody solution (0.5 % Triton X-100, 0.9 % sodium chloride, 1% FBS in PBS) for 2 nights in agitation at 4°C. To ensure the complete excess removal, the samples were rinsed with 0.1% v/v Triton X-100 in PBS (twice for 10 minutes) and after they were incubated with the secondary antibody (donkey anti-goat 1:200) in a secondary antibody solution (0.5% Triton X-100, 0.9% Sodium Chloride, 1% FBS in PBS) for 1 hour at room temperature in the dark. Finally, the retinas were rinsed with PBS three times for 5 minutes and were then stained with DAPI (1:5000) for 5 minutes. After the rinsing with PBS twice for 5

minutes, the retinas were mounted between two cover slips and stored overnight at 4°C. The samples were analysed with an Olympus microscope (Rungis, France). Brn3a cells number was determined manually using the cell counter in ImageJ Software in the central, mid-peripheral and peripheral retinal regions and statistics were calculated using Prism GraphPad. 8.0.2.

3.25 Statistical analysis

Statistical analysis was performed using GraphPad Prism 8.0.3 software. Statistical significance was defined at $*p < 0.05$, $**p < 0.01$, and $***p < 0.001$ by using one-way ANOVA with Dunn's testing for post-hoc comparisons or the standard Student t test. All results are presented as mean ± standard error of the mean (SEM).

Chapter 4

RESULTS

Chapter 4

4. Results

4.1 Microparticles characterization

The morphology of the microspheres was evaluated by Scanning Electron Microscopy (SEM) (Fig. 2). In all the produced formulations, spherical particles were obtained. Interestingly, the presence of poloxamers in the organic phase of the emulsion, even in a low amount (0.5:0.5:9 F68:F127:PLGA weight ratio) had a fundamental impact on the resulting particle morphology. Indeed, the surface of poloxamers-containing MP formulations was smooth and non-porous (Figs. 6A, 6B, 6D, 6E), while a close-up examination revealed evident surface pores in the case of MPs consisting of PLGA only (Figs. 6C, 6F).

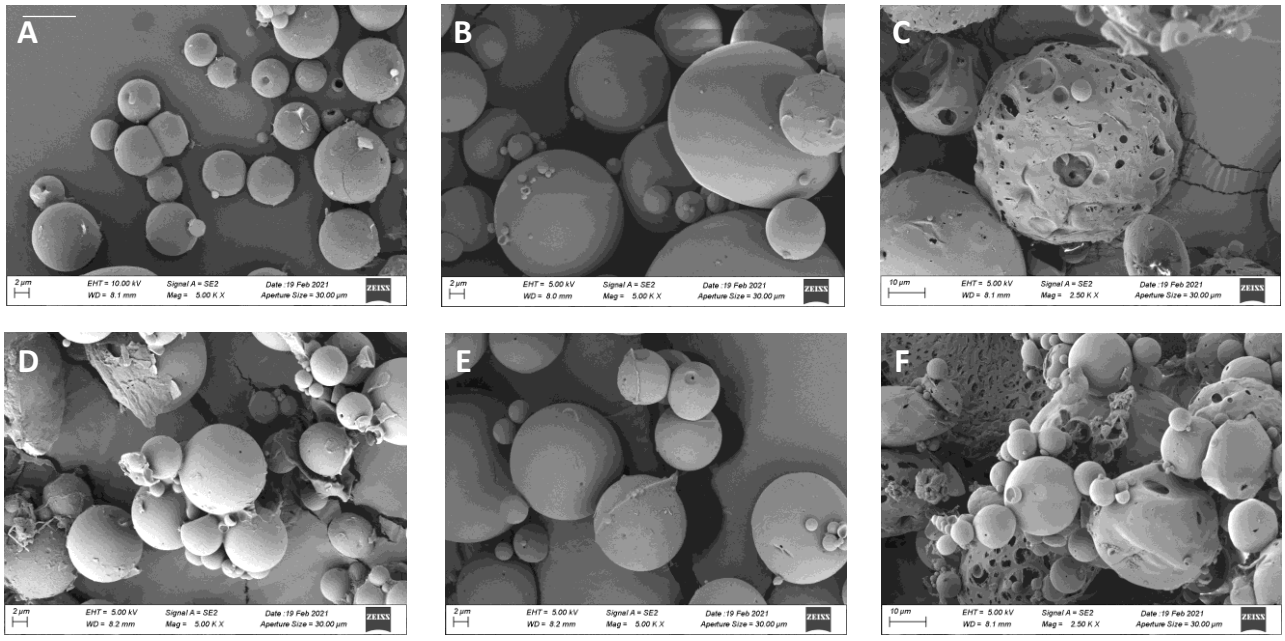

Figure 6. SEM images of (A) 20-70 (B) 20-90 and (C) 20-100 (D) 24-70 (E) 24-90 and (F) 24-100 MPs. The bar is 2 μm in (A), (B), (D), (E) and 10 μm in (C) and (F).

The mean diameter, BSA entrapment efficiency and yield of the obtained formulations are reported in the following Table 8. The table and SEM images indicate that size of control, PLGA-only MPs

was higher at both polymer concentrations, while the mean diameter was 14-15 μm in all the other cases.

Table 8. Overall technological features of the produced MPs. The results were expressed as the mean value ± SD calculated on at least three repeats.

Formulation	Mean diameter [μm] (± SD)	E.E. [%] + (± SD)	Yield + (± SD)
20-100	30 ± 8.4	49 ± 4.0	27 ±12
20-90	14 ± 6.0	63 ± 13	38 ±10
20-70	14 ± 6.0	43 ± 1.0	43 ± 24
24-100	31 ± 5.0	61 ± 10	30 ± 15
24-90	15 ± 7.0	68 ± 19	35 ± 21
24-70	15 ± 6.2	81 ± 18	27 ± 15

Protein encapsulation efficiency (EE) was between 43 and 81% in all cases, as shown in Table 8. In particular, EE was found to be significantly higher when overall polymer concentration in the organic phase was 24% w/v. Yield values were 27-43% in all cases.

In the case of MPs loaded with PEA, Citicoline and GDNF, the mean diameter was higher (26-39 μm) even if the production technique was the same, while EE was widely variable, between 9 and 68%, as summarized in Table 9.

Table 9. Summary of technological features of unloaded and loaded MPs with PEA, Citicoline and GDNF. The results were expressed as the mean value ± SD calculated on at least three repeats.

Formulation	Mean Diameter (μm) ± SD	EE (%) ± DS	Yield % ± DS
MP Citicoline	28 ± 2.0	19 ± 8.0	31 ± 2.0
MP PEA	26 ± 3.0	9.0 ± 6.0	26 ± 4.0
MP GDNF	39 ± 6.0	68 ± 5.0	14 ± 7.0

4.2 Diffusion studies of fluorescent MPs

The results of the diffusion tests of fluorescent microparticles made up of only PLGA, MPs decorated with HA 180 kDa and MP decorated with HA 1600 kDa, are shown, respectively, in Figures 8-10.

Actually, MP size exceeds the vitreous mesh size (about 500 nm) [71] and this clearly discourages their free diffusion into the posterior segment of the eye. Specifically, MP transport through the viscous vitreous body requires the widening of the mesh of the hydrogel constituting the vitreous body.

The SVB was prepared according to the procedures reported in the literature and, before the release and diffusion studies, it was verified that its rheological properties were close to those of the human vitreous body. In Figure 7, the storage and loss moduli of the produced SVB is reported as a function of the testing frequency, in the range 0.1–10 Hz. Both G′ and G″ range from low values up to approximately 20 Pa and show an increasing trend with frequency. Comparison with the experimental data relative to the human vitreous humor reveals that the rheological spectra lie within the appropriate range, with similar trend of the rheological moduli [67] [72].

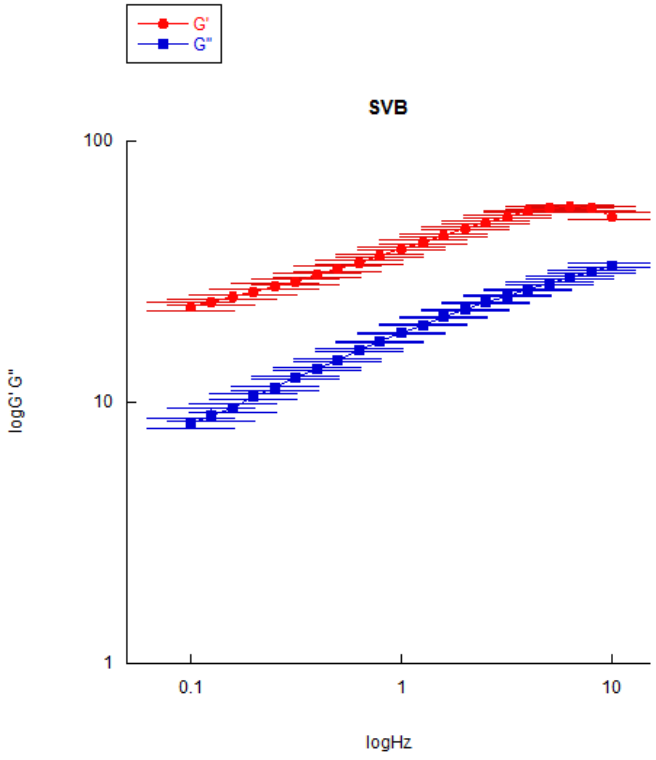

Figure 7. Rheological analysis of SVB at 37 °C. Results are expressed as mean values ± the standard deviations calculated over three replicas.

Hereafter, the syringe technique was used to evaluate transport properties of MPs into SVB, thus mimicking their sedimentation after the intravitreal injection of MPs. More in detail, diffusion tests of fluorescent HA1600 and HA180 MPs in SVB were performed and compared to the transport properties of MPs without HA corona (namely PLGA MPs) of comparable size. Results of diffusion tests are presented in figures 8, 9 and 10.

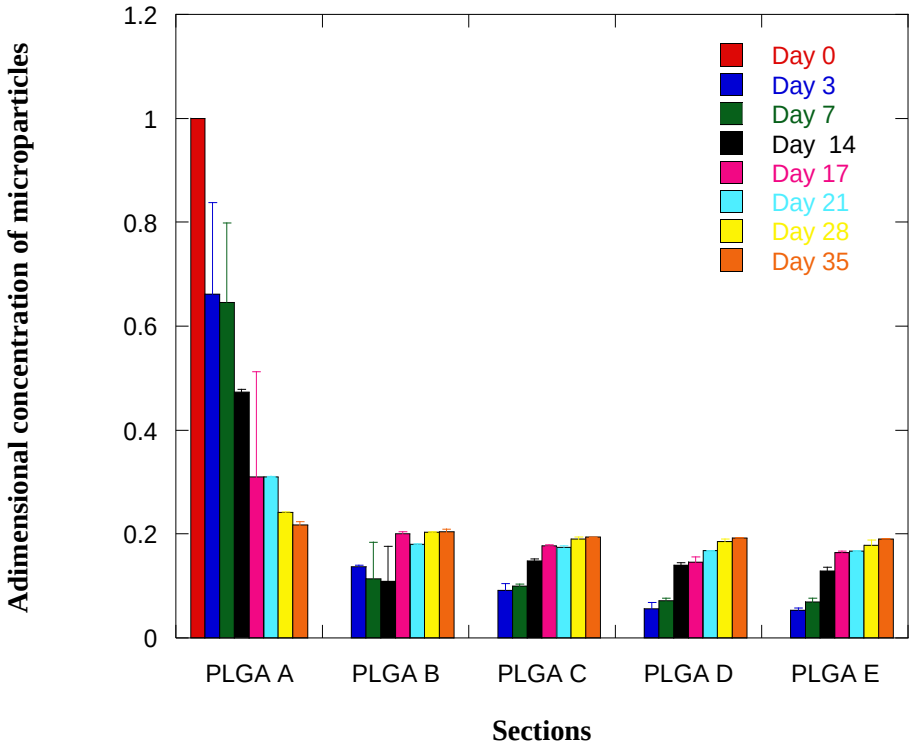

Figure 8. Diffusion test of control PLGA MPs.

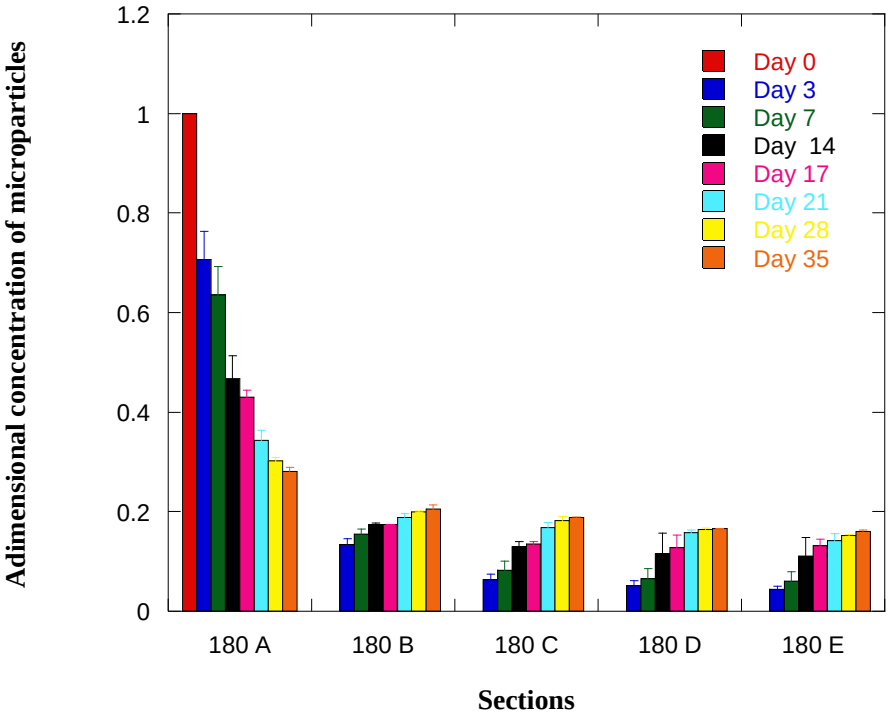

Figure 9. Diffusion test of HA180 MPs.

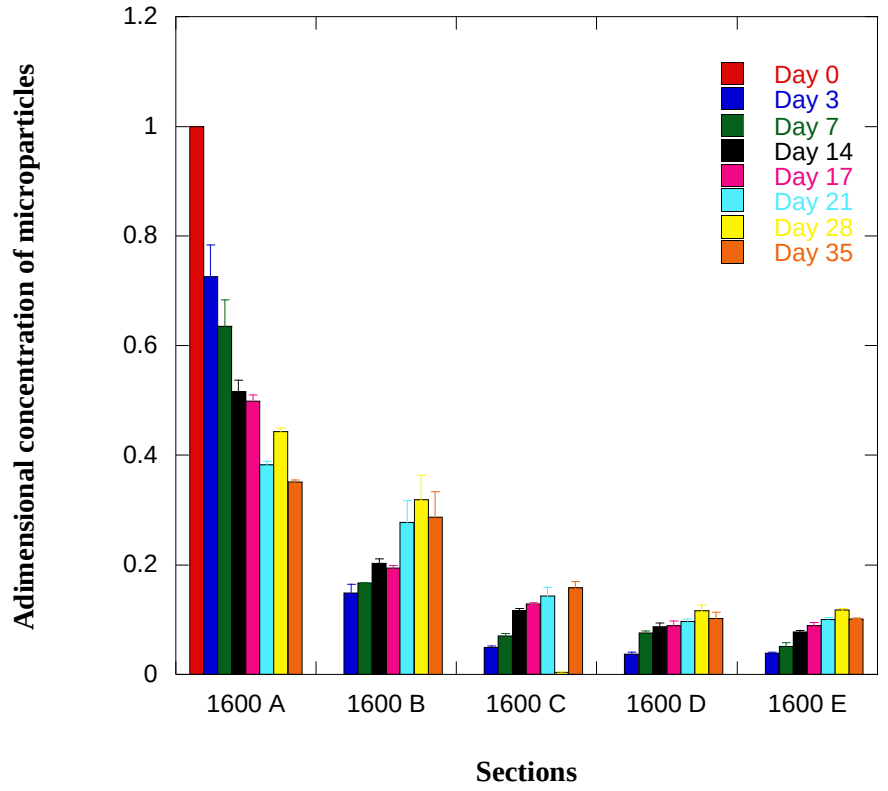

Figure 10. Diffusion test of HA1600 MPs.

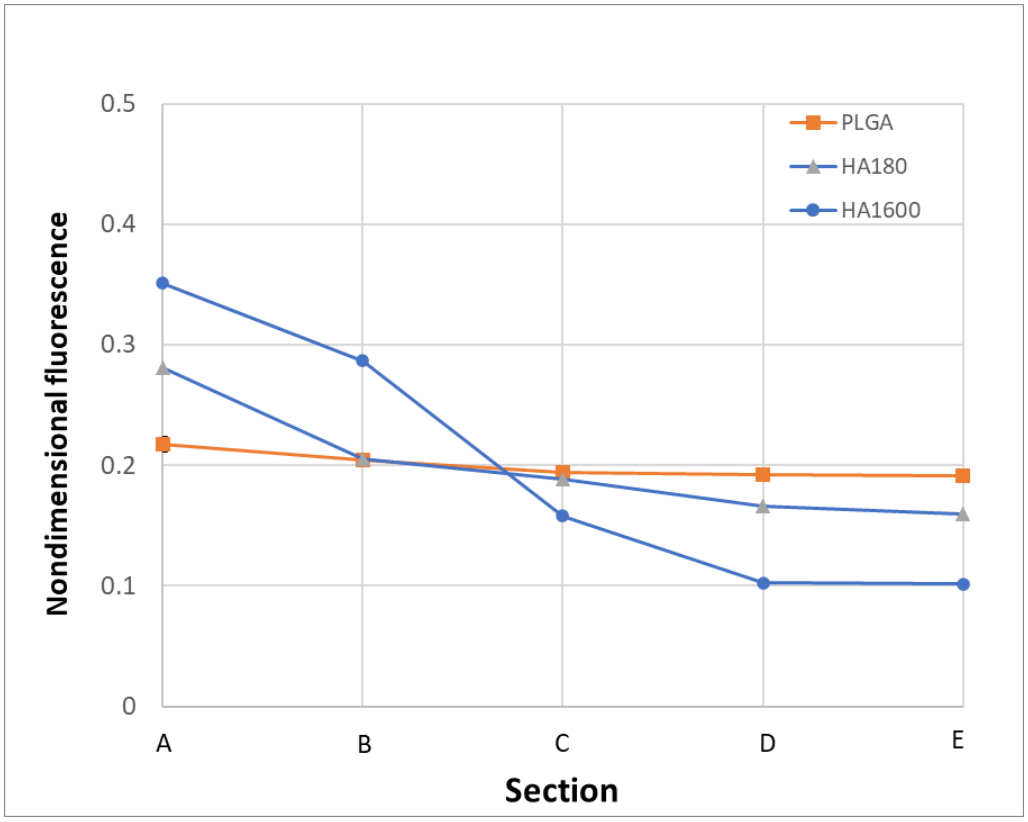

Figure 11. Results of diffusion experiments after 35 days for PLGA, HA 180 and HA1600 MPs.

The obtained results have shown that, in time, a higher percentage of HA1600 MPs can be found in the first section of the syringe. More in detail, after 35 days, bare PLGA MPs diffuse from section A of the syringe (in which the MPs were initially loaded) to section E and are uniformly distributed thought the syringe sections. In the case of HA180 and HA1600 MPs, approximately 28 and 35% of the fluorescence was determined in the first section. Differently, in section E there are ~16% and ~10% of HA180 and HA1600 MPs initially loaded in section A, respectively.

4.3 Release studies of MPs in SVB

In order to study the release features of the produced MPs decorated with HA in the ocular vitreous body, control PLGA and HA-decorated MPs have been dispersed in SVB and the resulting MP-loaded gel placed on the bottom of a vial, covered with PBS and incubated at 37 °C. The presence of SVB

ensures the interactions between the HA chains exposed upon MPs surface and the HA molecules contained in SVB. At scheduled time points, spectrophotometric analysis has allowed to assess whether the molecular weight of HA coronas influenced drug release kinetics of BSA from MPs. In figure 12, the release profiles of BSA from PLGA-based MPs, with or without external HA (at 180 or 1600 kDa) corona, are reported.

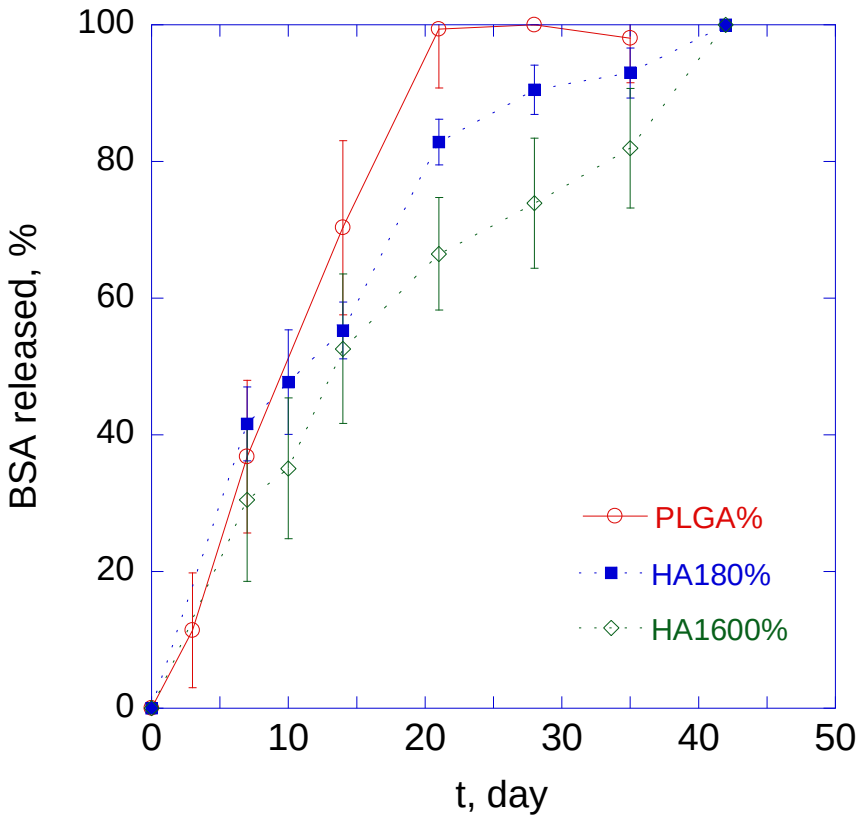

Figure 12. Temporal release trends of BSA from MPs over time.

It is known that drug release from PLGA-based drug delivery systems is governed by a complex mechanism deriving from the combination of drug diffusion through the polymeric matrix and the concomitant polymer bulk degradation [73]. Results indicate that PLGA MPs can prolong BSA release phase for three weeks with a release curve which is, in this time frame, basically superimposable to that obtained from MPs decorated with HA 1600 kDa (HA1600) and slower

compared to MPs decorated with HA 180 kDa (HA180). Differently, both formulations containing HA present qualitatively similar trends of protein release kinetics, with a prolonged release phase for at least six weeks. Specifically, the amount of protein released by HA1600 MPs was found to be lower compared to that released by HA180. Therefore, a prolonged degradation time of MPs, due to the presence of poloxamers in the formulation, contribute to sustain the release of the loaded drug molecule(s), thereby reducing the frequency of intravitreal injections and the related risk of adverse effects.

In order to evaluate the influence of poloxamers presence not only on degradation rate but also on drug release kinetics, several batches of MPs with different overall polymer concentration and PLGA/poloxamers ratios were investigated to this aim. All MP formulations were decorated externally with HA 1600 kDa, which had been shown to sustain protein release more effectively and was consequently chosen as the constituent of MPs corona for the forthcoming studies.

In vitro release profiles of BSA from the produced MPs in SVB, along with the results of numerical simulations, are shown in Figure 13 and 14. When polymer concentration in the organic phase of the emulsion was 20% w/v, the presence of poloxamers influenced protein release kinetics. Indeed, 20-100 formulation showed a considerable initial burst. The residual protein discharge was sustained for 4 weeks. In the case of 20-90 MPs, BSA was released in a similar time, but with a very attenuated burst effect. Protein release from the 20-70 MPs was found to be unsatisfactorily reproducible, as indicated by the high standard deviations.

Likewise, BSA release profiles from 24-90 and 24-100 formulations were essentially similar, with a complete delivery within 4 weeks while, in the case of 24-70 formulation, protein discharging was slightly quicker. Interestingly, no substantial burst was detected for 24-70, 24-90 and 24-100 formulations, while a moderate acceleration of protein release was seen between 7 and 14 days, which

implies that considerable fractions of bulk BSA are present for these formulations in the specified time frame.

The released fraction of BSA from the different MP formulations was modeled as described in *Section 3.11* and the best fit parameters are summarized in Table 10. The values of the solubilization rate constant k_S were pretty close for all formulations, which indicates that superficial phenomena within MPs during release are comparable irrespective of polymer concentration and poloxamers presence.

However, when polymer concentration was 20% w/v in the organic phase of the emulsion, $\varphi_{S,\infty}$ was increasing with increasing PLGA:poloxamers ratio. As for MPs produced with 24% w/v polymer concentration in the organic phase of the emulsion, no clear trend of $\varphi_{S,\infty}$ with poloxamers percentage was seen, indicating that the high polymer concentration is associated to a dense MP matrix which effectively hampers BSA diffusion and subsequent release.

The t_{MAX} values were around 10-12 days for all formulations, while being higher in the case of 24-70 MPs (14 days). In this latter case, the higher erosion rate described by k_E is associated with a longer time corresponding to the maximum erosion rate.

Table 10. Best fit results of BSA release kinetics modelling for the six MP formulations.

	20-70	**20-90**	**20-100**	**24-70**	**24-90**	**24-100**
k_S [day^{-1}]	4.60	4.41	4.86	4.40	4.33	4.33
$\varphi_{S,\infty}$	0.031	0.089	0.429	0.204	0.080	0.146
k_E [day^{-1}]	0.234	0.241	0.202	0.391	0.262	0.229
t_{MAX} [day]	9.78	11.7	9.89	14.0	11.0	11.5

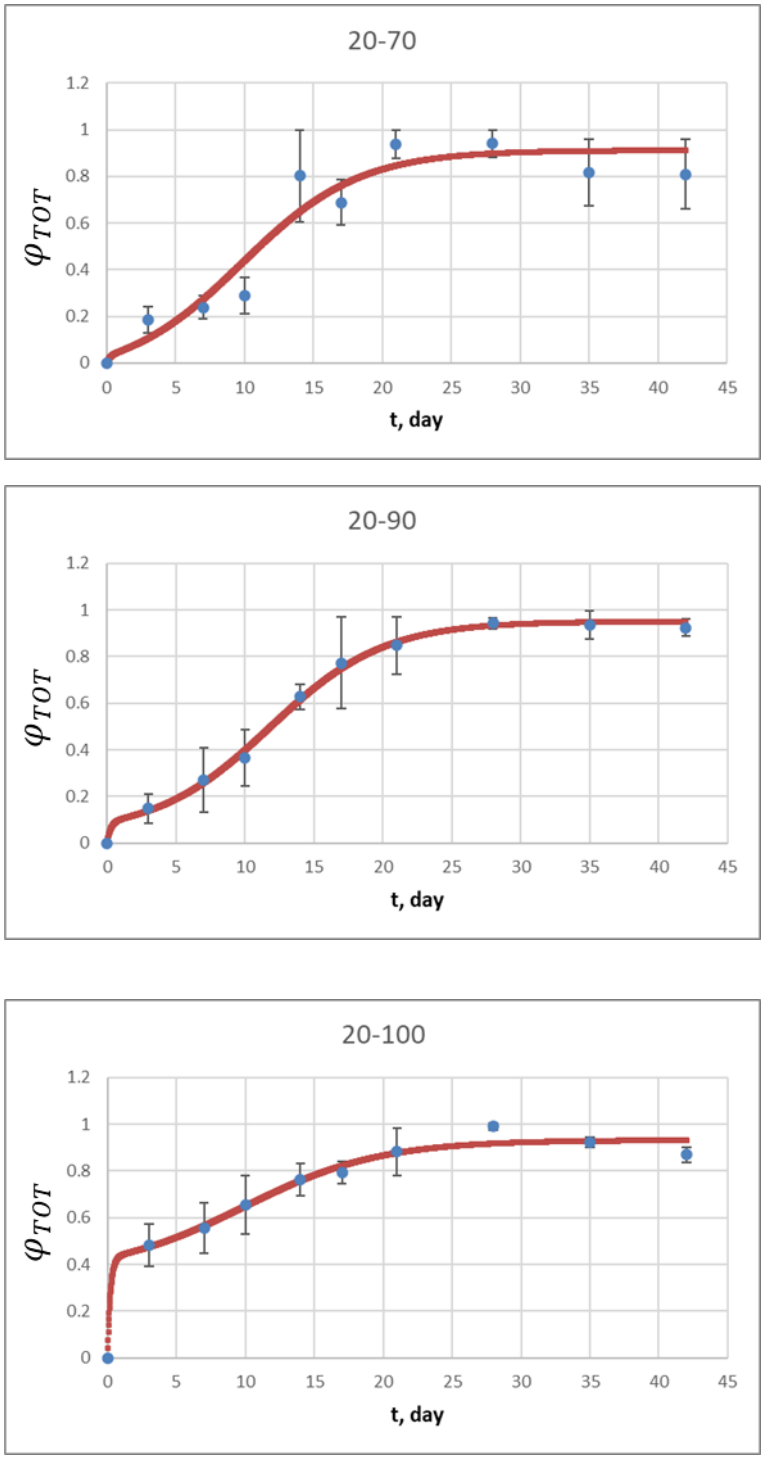

Figure 13. *In vitro* protein release kinetics from PLGA-based microparticles at 20% w/v overall polymer content in the organic phase of the emulsion. Solid lines represent numerical simulations.

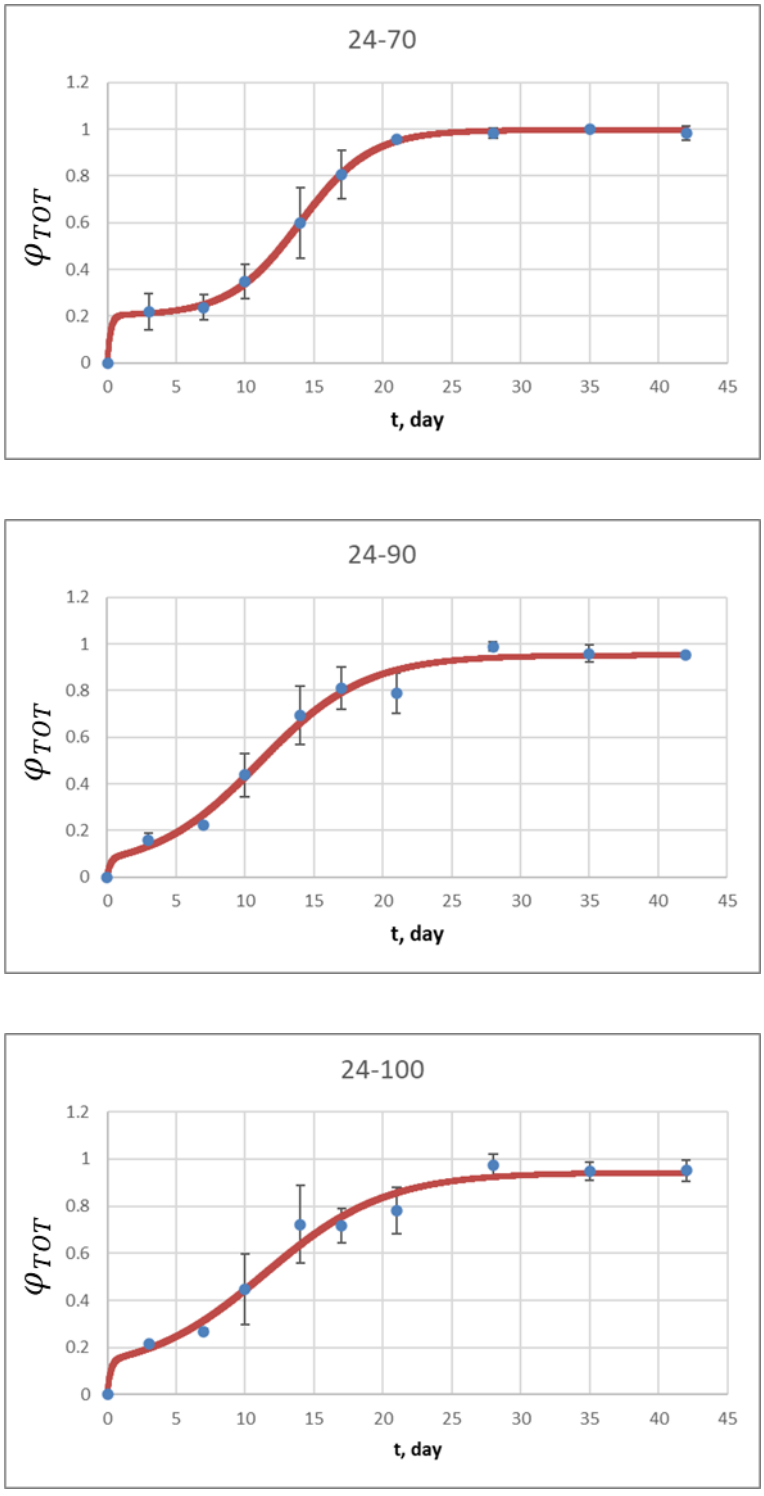

Figure 14. *In vitro* protein release kinetics from PLGA-based microparticles at 24% w/v overall polymer content in the organic phase of the emulsion. Solid lines represent numerical simulations.

4.4 Degradation studies of MPs

As described in the Section *3.12*, the mass loss/degradation kinetics have been observed through a 0.5% w/v MPs suspension in PBS incubated at 37°C. At scheduled time points, the residual mass of the MPs was gravimetrically obtained on the lyophilized residue, taking into account the mass of salts.

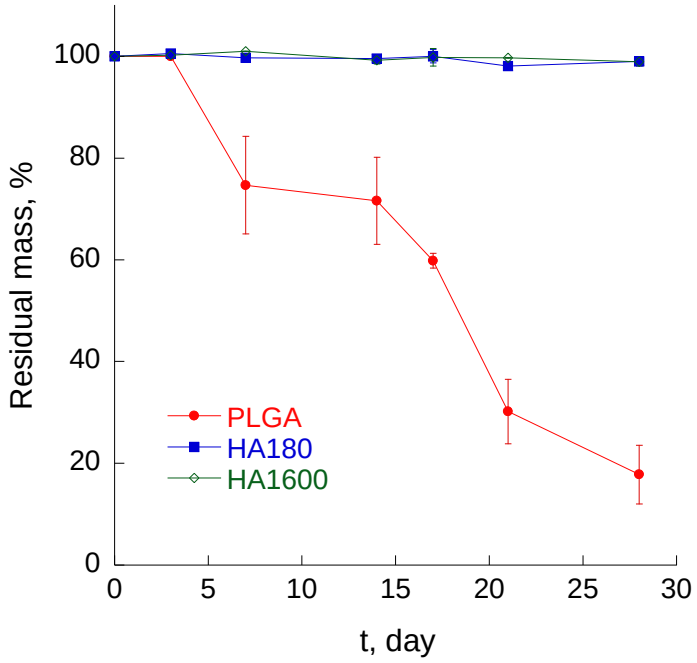

Figure 15. MP time trend of mass loss.

Percent changes in MP mass were calculated as the rate of material loss during the incubation of the devices over a 4-week course *in vitro*. The trend of MP mass loss is presented in Figure 15.

The collected data display that in 28 days control PLGA MPs lost > 80% of their initial mass while, in the same time frame, the overall mass of both HA-containing formulations was roughly constant, with a loss of material around few per cent points, therefore showing a decisive effect of poloxamers in dictating the rate of MP degradation and dissolution.

This indicates that, only in HA-containing devices, the molecular weight of PLGA is still above the dissolution threshold value and, hence, that the degradation rate for both formulations is definitely lower.

4.5 GPC analysis

Table 6 reports the molecular weight distributions, intrinsic viscosity (IV) and weight fraction of polymeric part, named peak 1, ranging from 9 to 15 min retention volume, and low molecular weight fraction comprehensive of degraded chains (oligomers, monomers, etc.), named peak 2 ranging 17.5-19 min retention volume (Figure 16). It is important to underline that the values reported (Mw, Mn and IV) must be accounted to a mix of undegradable poloxamers and PLGA.

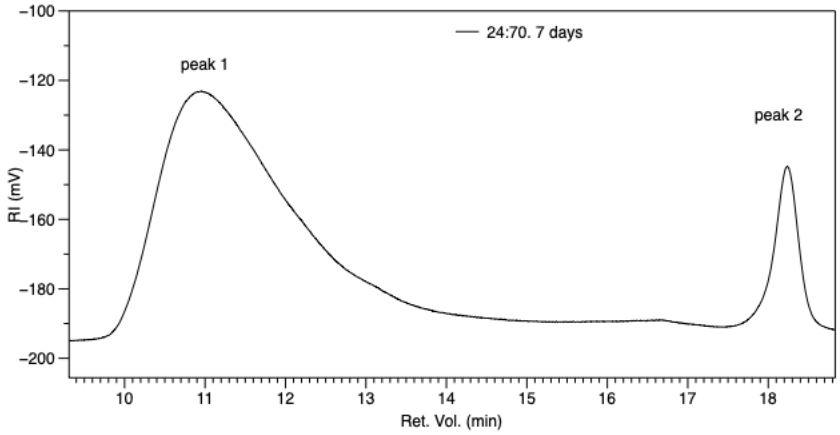

Figure 16. Representative GPC chromatogram at RI detector showing peak 1 and peak 2

Table 11. Weight-average molecular weight (Mw), number-average molecular weight (Mn), intrinsic viscosity (IV) and weight fraction of peak1 and peak2 as determined by GPC.

Entry	Sample	Mw (Da)	Mn(Da)	IV	%wt.peak 1	%wt.peak 2
1	20:100 7d	34266	15372	0.193	87	13
2	20:100 14d	24741	7648	0.208	75	25
3	20:100 21d	22545	8206	0.185	69	31
4	20:100 28d	19953	6350	0.143	34	66
5	20:90 7d	31576	10592	0.206	78	22
6	20:90 14d	20305*	9269*	0.150	66	34
7	20:90 21d	21108	7759	0.152	83	17
8	20:90 28d	17035	8238	0.216	21	78
9	20:70 7d	27449	9922	0.178	78	22
10	20:70 14d	21027*	9245*	0.150*	76	24
11	20:70 21d	22581	9032	0.126	82	18
12	20:70 28d	20213	7646	0.149	53	47
13	24:100 7d	31596	13596	0.207	85	15
14	24:100 14d	23282	7861	0.206	78	22
15	24:100 21d	20963	7403	0.156	73	27
16	24:100 28d	15817	6160	0.125	51	49
17	24:90 7d	27233*	10883*	0.201	74	26
18	24:90 14d	24703	8440	0.127	74	26
19	24:90 21d	11053	4141	0.132	46	54
20	24:90 28d	9545	4150	0.104	43	57
21	24:70 7d	26919	7522	0.199	86	14
22	24:70 14d	20847	6120	0.164	72	28
23	24:70 21d	14143	4922	0.136	75	25
24	24:70 28d	14217	4718	0.132	43	57

Comparing 20 –100 and 24 – 100 series, it is possible to note that molecular weights and IV decrease overtime with the same trend (Figure 16), as expected due to the similar porous appearance of MPs (see Figure 6). Instead, the ratio between peak 1 and peak 2 is different, possibly due to major amount of degraded PLGA (entries 4 and 16 in Table 11).

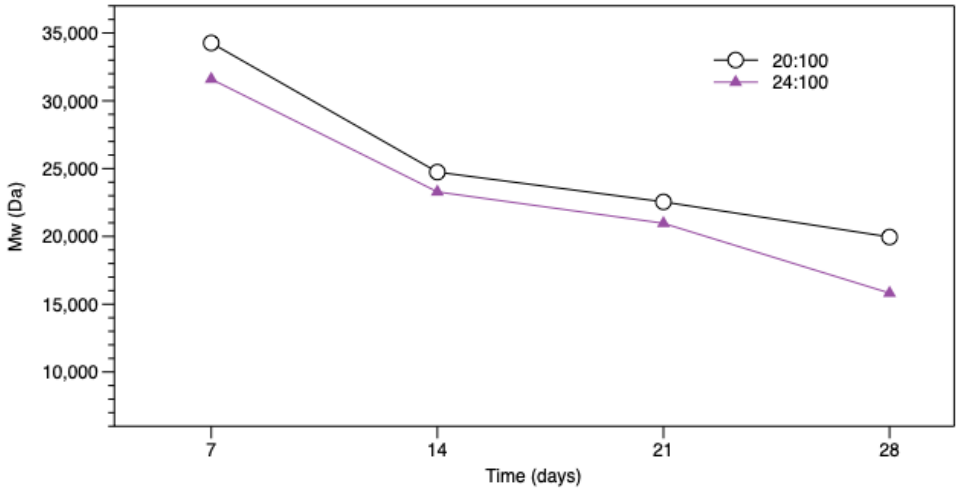

Figure 17. Time trend of for 20-100 and 24-100 (PLGA – only) MPs

In any series, except 24 – 100, after 14 days PLGA decomposes significantly slower, and this outcome is in line with release kinetics and burst release data.

In the 20 – 90 series, it is possible to note that Mw is roughly half of its initial value at the final point and, at the same time point, IV is higher than previous samples, with a value close to pure poloxamer F127. This could be explained figuring a peak 1 (9-15 min retention volume) composed mainly by poloxamers as consequence of "high" degradation rate of PLGA. This may indicate that poloxamers cannot exert a satisfactory "shielding effect" due to their low amount in 20-90 formulation. This hypothesis is supported by values of peak 1 and peak 2.

In the 20 – 70 series, the higher concentration of poloxamers lead to a "slower" degradation, as indicated by peaks 1 and 2, however at final point IV slight increase out of the trend, showing a not excellent protection of PLGA from degradation.

In 24 – 90 and 24 – 70 series, the higher concentration of polymers leads to lower molecular weights at starting points. In both series and more evident in 24 – 70 series it is possible to see (Figure 18) the presence of poloxamers in peak 1 at 14, 21 and 28 days and at the last point it is possible to note a shoulder at 10.3 min attributable to non-degraded PLGA.

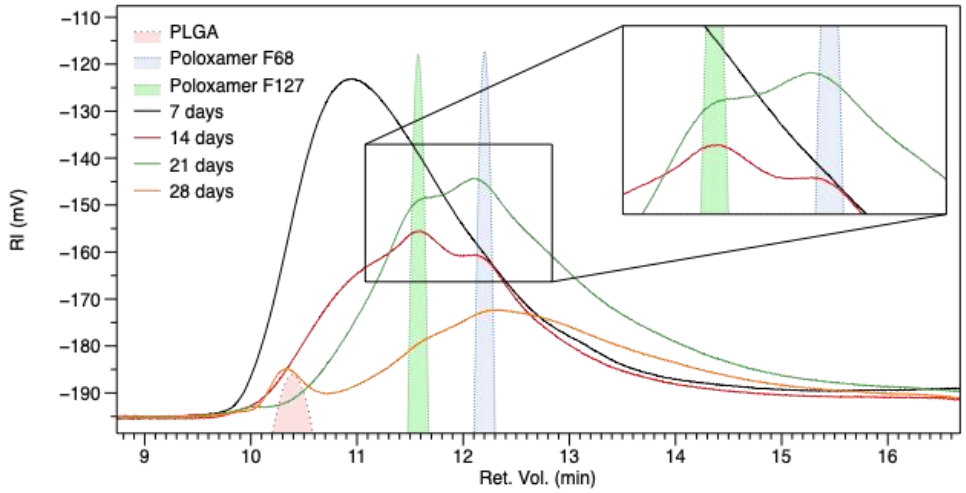

Figure 18. Superimposed chromatograms at RI detector of 24:70 series and in full red pure PLGA, in full green poloxamer F127, in full blue poloxamer F68. Chromatograms from 14 days show the presence of poloxamers and at 28 days a residual peak of PLGA.

4.6 Differential Scanning Calorimetry

The thermograms of raw PLGA, poloxamers and of just produced MPs are summarized in Figure 19. As displayed in Figure 19A, the thermogram of PLGA shows a glass transition temperature (Tg) around 49°C, while F68 and F127 poloxamers exhibited an endothermic melting peak at about 54 and 56°C (Figure 19B and 19C). DSC traces of HA showed no thermodynamic events in the test conditions (data not shown). Similarly, also MPs did not show the endothermic peaks of poloxamers, thereby indicating that they are molecularly mixed with PLGA.

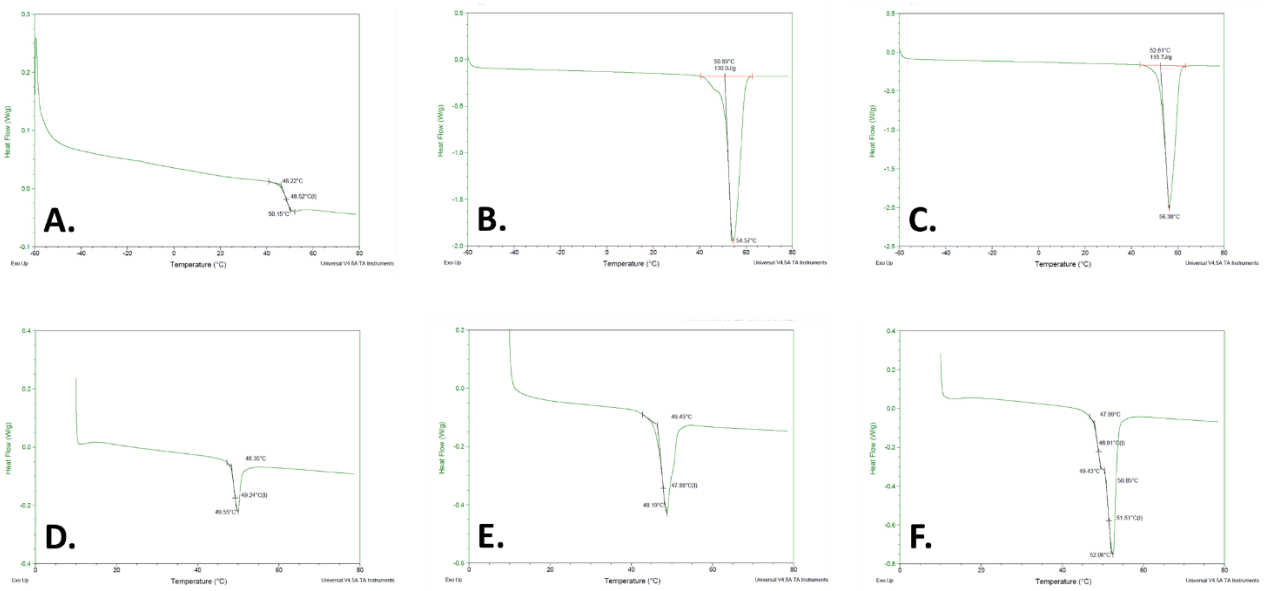

Figure 19. DSC thermograms of PLGA powder (A); F68 poloxamers powder (B); F127 poloxamers powder (C); 20-100 (D), 20-90 (E), 20-70 (F) microparticles.

Figure 19 shows the representative DSC traces of pure materials and of the as-produced 20-100, 20-90 and 20-70 MPs. HA did not show any thermal event in the utilized temperature range (data not shown). PLGA showed only a glass transition around 48°C (Figure 19A), with no crystallinity or fusion due to its amorphous nature, while F68 and F 127 poloxamers evidenced a relatively sharp endothermic peak attributed to polymer melting (Figure 19B and 1C, respectively).

Figure 14 depicts the time trend of Tg for all formulations, until day 28. Glass transition temperature was found to follow a slowly decreasing time trend, substantially superimposable for all MP formulations. Tg was steadily decreasing until day 28, dropping from approximately 49 to 42°C, due to the drop pf PLGA molecular weight during release.

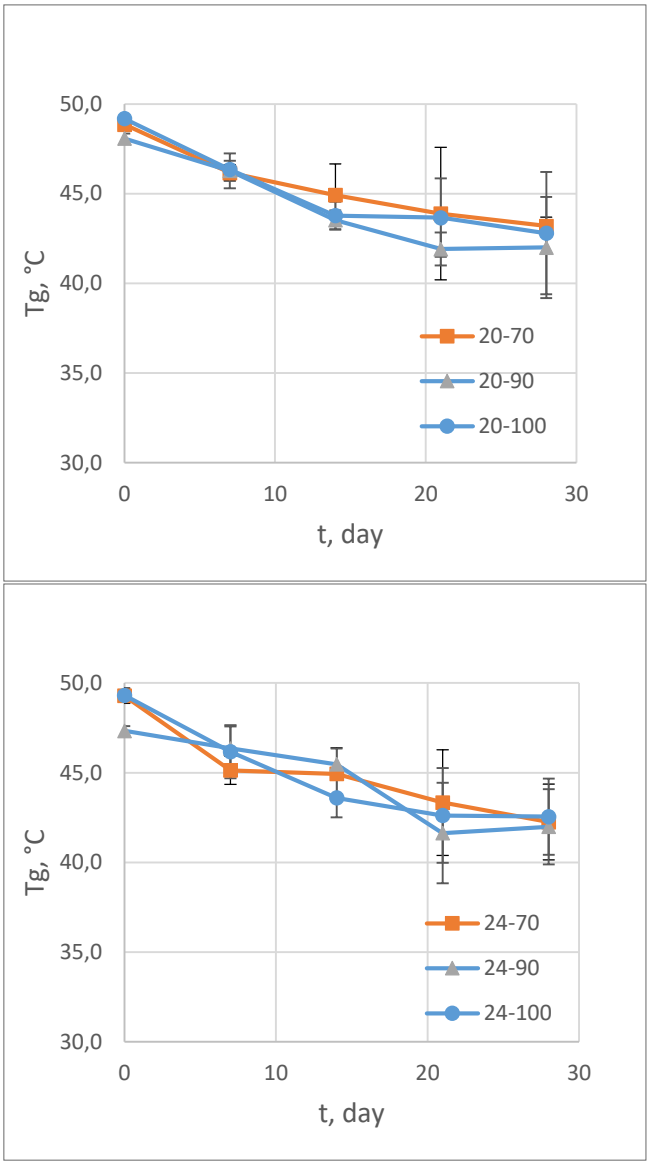

Figure 20. Trends of PLGA glass transition temperatures for the six formulations.

Chapter 5

DISCUSSIONS

Chapter 5

5. Discussions

In this study, biodegradable PLGA-based microspheres intended for intravitreal injection were designed and fabricated. HA was chosen as for the external MP decoration since it was here hypothesized that this would reduce MP propensity to freely diffuse in the eye. Moreover, MPs were formulated to sustain the drug release phase; in a possible clinical application, this may in principle allow a reduction of the frequency of intravitreal injections. This is in turn associated to a possible decrement of developing the unwanted side effects of the injection [16].

The MPs decorated with HA were produced by a slightly modified double emulsion – solvent evaporation technique, as described in the *Materials and Methods* chapter. HA was added to the external aqueous phase to promote its interaction with the organic phase containing the blend of lipophilic PLGA and amphiphilic poloxamers. During the second emulsification step, the hydrophilic segments of the poloxamers within the droplets of the internal organic solution spontaneously orient towards the external aqueous phase containing HA. This is expected to be decisive in promoting the HA arrangement on the surface of the MPs, driven by the lipophilicity gradient between the organic and the aqueous phase of the emulsion [65], after the evaporation of the organic solvent. Specifically, HA was chosen because it is a major component of the vitreous body, and this is expected to increase MPs affinity with the surrounding gel containing the same polysaccharide. In this work, it has been hypothesized that this affinity of composition between the surface of the MPs and the vitreous body may hinder the diffusion/sedimentation and aggregation of MPs within the ocular vitreous. A further objective of this work was to evaluate if the molecular weight of the HA used to decorate the surface can influence the degradation and diffusion of the MP in the simulated vitreous body (SVB), as well as the release kinetics of the loaded protein. It must be underlined that, for a possible clinical application, the site of injection of MPs must be properly chosen to avoid the risk of vision blurring. Regarding this, it was explored the intravitreal injection on rat models by performing it in a specific

site of the ocular globe, that is the superior pole. After the animal euthanasia, the eye was enucleated with a piece of tissue at the superior pole, in order to orient the eye after the explant and to be better recognize it. Indeed, the microscope analysis had led us to clearly identify the site of injection and the MPs presence nearby. In this perspective, a successful treatment based on intravitreal MPs injection is strictly related on MPs injection outside the visual path within the eye. For this reason, negligible diffusion features of MPs in the long time are necessary to ensure a significance of the treatment [79].

A detailed discussion of the findings is reported in the following sections.

5.1 Effect of poloxamers on physicochemical properties of MPs

The morphological analysis by SEM have shown that the poloxamers presence play a relevant role in homogenization process. Indeed, MPs whose organic phase contains poloxamers present a smooth and non-porous surface. This underlines the bridging role of poloxamers between PLGA and HA which enhances the formation of a more uniform polymeric matrix in MPs.

Actually, the data currently available suggest a formation of a lipophilic/amphiphilic internal phase, which is associated to a relatively continuous change of affinity between the internal and external phases of the emulsion used to produce the MPs. Importantly, this can also be correlated to the lower mean diameters of MPs containing poloxamers (Figure 6, Table 8). In actual fact, an increased affinity between the phases of the emulsion, due to the presence of poloxamers, can be associated to smaller droplets and, finally to smaller MPs. As a matter of fact, the average diameter of the MPs made up of PLGA alone was around 30 μm, while in the presence of the poloxamers MPs of 14-15 μm are obtained.

The increasing EE values with higher polymer concentration can be reasonably explained considering that the higher polymer concentration leads to an increase in the viscosity of the organic

phase of the emulsion and therefore a reduced shear stress during the emulsion. This is reasonably associated to a discouraged migration of BSA towards the external aqueous phase and, overall, an increased EE of the protein.

The influence of poloxamers presence can be observed also on degradation rate. In detail, autocatalytic PLGA degradation can be schematized as follows: (i) initially, water invades the polymeric matrix due to MP porous structure which allows a fast water penetration [14] and polymer plasticization [73]; (ii) then, hydrolysis-triggered PLGA degradation at chain backbone takes place and, progressively, soluble acidic by-products are formed when the molecular weight reached the solubilization threshold; (iii) the produced acids catalyze degradation, thereby furthering the formation of additional soluble acidic degradation products [80]. It must be specified that, during degradation, molecular weight steadily decreases, while device mass loss takes place when polymer molecules reach a critical molecular weight below which PLGA oligomers are soluble. Actually, poloxamers presence in the bulk of MPs is associated to a dilution of acidic degradation products, along with a buffering effect which slow down the autocatalytic degradation of MPs. Furthermore, it must be pointed out that MPs containing poloxamers are more hydrophilic compared to the devices made up of bare PLGA and this enhances the diffusion of acidic degradation by-products outwards to the surrounding gel. Furthermore, the results depicted in Figure 12 indicate that different molecular weights of HA molecules on MP surface has seemingly no effect on the advancement of PLGA degradation in this first stage of HA containing MP degradation.

More specifically, the decrease of overall MPs molecular weight in the absence of poloxamers was faster for 24–100 compared to 20–100 formulations. This indicates that, despite the porous morphology of microdevices, autocatalysis is somehow enhanced at the highest polymer concentration in the organic phase of the emulsion. Specifically, 20-90 and 24-90 MPs showed a somewhat increased degradation rate, at a higher extent in the case of 24-90 formulation. This can be explained considering that poloxamers facilitate water penetration, with autocatalysis being very

likely due to high polymer concentration. Consequently, the formation of short PLGA chains in MPs bulk is promoted by enhanced water penetration, while the transport of degradation products is hampered. At the same time, the increased MPs hydrophilicity is expected to facilitate base penetration in MP, which neutralize the generated acids. The overall balance suggests that acid generation is probably faster than the neutralization [81] [82] which is related to a drop in local pH within MPs.

The presence of higher poloxamers concentration in 20-70 and 24-70 MPs, on the contrary, induced a degradation rate closer to that of 20-100 and 24-100 MPs. Actually, higher poloxamer amounts are expected to promote water intrusion in MPs, and this in turn causes an enhanced mobilization of the acidic degradation products of PLGA. Accordingly, the decrease of pH in MPs bulk is probably less marked, resulting in a slightly discouraged autocatalysis compared to 20-90 and 24-90 formulations. This mildly impacts BSA release profiles (Figure 13 and 14). It must be underlined that BSA mobilization is dictated by the complex hydrophilicity/hydrophobicity interplay which is in turn affected by changing PLGA molecular weight and poloxamers solubilization. Indeed, a lower molecular weight of PLGA results in promoted BSA transport and increased polymer hydrophilicity due to an increased number of carboxylic groups *per* mass unit. The increased hydrophilicity associated to higher poloxamers weight ratios has different conflicting consequences: (i) it causes an enhancement in BSA mobility; (ii) MPs erosion is promoted by the leaking of degradation products and soluble moieties in the surrounding gel, leading to the formation of new pores; (iii) autocatalysis is discouraged due to the loss of soluble acids. All in all, the effect of poloxamers in MPs inner regions induced different overall effects on BSA discharge, which are also affected by the total polymer concentration. Indeed, 20-100 formulation, whose organic phase is made up in the absence of poloxamers, showed an remarkable initial burst, which can be attributed to the porous surface of MPs. The extent of burst effect affected also $\varphi_{S,\infty}$ which increased with increasing PLGA:poloxamers ratio

and this is consistent with the strong burst observed in 20-100 formulation. This outcome indicates that the release mechanism is mainly erosion-driven.

It should also be emphasized that poloxamers have two contrasting effects on MPs degradation/erosion. On the one hand, they increase the hydrophilicity of MPs, favoring their erosion; on the other hand, they dilute the PLGA reducing the autocatalytic effects, and therefore hindering erosion. The k_E values of the best fit indicate that for 20-70 and 20-90 MPs the two effects are roughly balanced. In the case of 24-70, 24-90 and 24-100 MPs, on the contrary, k_E values were descending as the percentage of PLGA increased. This indicates that, at the highest overall concentration of polymers, the effect of the promoted solubilization induced by poloxamers prevails in determining the erosion of MPs.

Remarkably, the thermograms of MPs displayed a glass transition event at temperatures close to the Tg of pure PLGA. In all cases, anyhow, glass transition event was overlapped with an endothermic peak attributable to poloxamers. It must be underlined that 20-100 MPs are produced with poloxamers in the external water phase, therefore the small endothermic peak observed is probably due to the poloxamers adhering to external MPs surface. As for 20-90 and 20-70 formulations, the endothermic peak is more relevant due to the increasing presence of poloxamers in the organic phase of the emulsion. These outcomes hint at the formation of a partially blended, phase-separated polymeric matrix in MPs, and also indicate the plasticizing effect of PLGA on poloxamers mixture. The same outcomes were found for 24-100, 24-90 and 24-70 formulations.

5.2 Effect of HA coating on MPs properties

The coating of MPs surface with HA, in the absence of a chemical reaction, is the main original contribution of this work. The data available to date also hint that HA presence and molecular weight play a role in the modulation of MPs free diffusion within the eye.

Indeed, the results of diffusion studies confirmed the hypothesis: MPs made up of bare PLGA diffuse in SVB faster than those decorated superficially with HA. At the end of the experiment a uniform fluorescence distribution was found out in all the sections of the syringe used for the transport studies. Additionally, by increasing the molecular weight of HA on MP corona, the diffusion of the microdevices from one section to another is further hampered. The different profiles of HA 180 and HA 1600 MPs suggest different arrangements of HA molecules of different molecular weight on MP surface. Indeed, high molecular weight HA is constituted by longer chains which can form physical entanglements. This feature may hinder the diffusion of the drug, thus slowing down drug release kinetics. The difference in diffusivity between MPs formulations can be confidently attributed to the presence of HA on the surface of MPs. In fact, it is possible to hypothesize that HA exposes the terminal of the polymeric chain outside the MPs, thus favoring the interactions with the simulated vitreous body, containing the same polysaccharide, and thus slowing down the transport of the MPs. Besides, the different conformations assumed by HA of different molecular weight affects both the number and the entities of the physical entanglements made with HA macromolecules present in the simulated vitreous, thus further modulating the diffusion kinetics of MPs. Therefore, HA1600 MPs, which is expected to expose longer HA chains on their surface, show a more hindered transport in SVB, compared to HA 180 kDa. This is likely to limit their aggregation once injected intravitreally, hence enhancing their ability to control and prolong drug release. It must be underlined that the diffusion tests were carried out under unfavorable conditions. Indeed, syringes were placed in vertical position; this entails a contribution of gravity which boosts MP transport.

HA was not shown any relevant influence on MPs degradation rate. Furthermore, the results depicted in Figure 15 show that the presence of different molecular weight HA molecules on the surface has seemingly no effect on the percentage of degradation in this first stage of HA containing MPs degradation. Consequently, this indicates that the control over MP degradation rate is dictated by the

bulk conditions of the devices, i.e., mainly to the interplay between poloxamers and PLGA in the polymeric blend constituting MP core.

Likewise, both formulations containing HA present qualitatively similar time trends of protein release kinetics, with a prolonged release phase for at least six weeks. Specifically, the amount of protein released from HA1600 MPs was found to be lower compared to that released by HA180. Therefore, a prolonged degradation time of MPs, due to the presence of poloxamers in the formulation, contribute to sustain the release of the loaded drug molecule(s), thereby reducing the frequency of intravitreal injections and the related risk of adverse effects. The different profile of HA 180 and HA 1600 MPs can be related to the HA arrangement on MP surface. Indeed, high molecular weight HA is made up of longer chains which can form physical entanglements. This feature may hinder the diffusion of the drug, thus slowing down drug release kinetics.

It must be highlighted that protein release from the produced MPs is relatively fast: BSA is completely discharged from MPs in the order of weeks. In principle, it seems a short period compared to the need to increase the time between two consecutive injections. Anyhow, the comparison must be made between the injection of a non-encapsulated drug as a bolus and the administration of MPs which are able to sustain the release for prolonged times. The in vivo outcome is the objective of the forthcoming results.

5.3 In vitro and in vivo studies for MPs safety assessment

In vitro and *in vivo* studies have been carried out to assess MP safety as drug delivery systems for posterior eye segments diseases. Drug-loaded MPs have been tested, using unloaded devices as a control. *In vitro* MTT assays and cytofluorometric analysis confirmed the MPs lack of cytotoxicity their safety ensuring a satisfactory cells viability. However, the neuroprotective effect was not so remarkable. This was also corroborated by *in vivo* studies on animal glaucoma model. In depth, the

retina histology was not affected by MPs intravitreal injection, as ONL, INL and segments thickness was roughly the same. Also, the immunohistochemical analysis confirmed the histology results since there were not detected any gliosis or inflammation throughout the retina. So, MPs did not induce morphological and functional alterations in the retina of the rats, therefore indicating a prosing safety profile of the produced drug delivery systems. This is an encouraging results in the view of a possible clinical application of the produced MPs.

On the other hand, the RCGs quantification showed that the neuroprotective effect elicited by MPs loaded with active molecules was not so notable. It is probably related to MPs vehicle trehalose solution, which has an effect on NMDA acute toxicity. Therefore, in this case, it is difficult to conclude on the protective effect of MPs. Further studies will concern the testing of MP protective effect on another models of glaucoma, such as chronic models of IOP induced by injection of microbeads in anterior chamber or optic nerve crush.

Even if MPs have the tendency to aggregate several days after IVT in small animals [4], [83], this phenomenon was not observed in the present study. Among the clinical signs, inflammation can occur in early stages after IVT of MPs. Previous studies explained it as a non-progressive foreign body reaction [83]. It is therefore improbable that additional inflammatory reaction can be observed subsequently. Recent works have shown that no inflammatory reaction occurred in rats when PLGA-based MPs completely degrade after intravitreal injection, except for the activation of retinal glial Müller cells [83]. In this study, anyway, no retinal and choroidal damage were observed seven days after administration. In humans, the special concern is related to the risk of visual impairment after intravitreal injection of MPs. This clinical issue has been previously evaluated in a tolerance study, in which sustained-release triamcinolone MPs systems was injected in human eyes. It was reported an aggregation behavior by MPs at the site of the injection leaving a free visual axis. In the same study, no inflammation was observed after MPs injection, although it must be taken into account that the anti-inflammatory drug triamcinolone played a role in attenuating the inflammatory reaction [84].

It must be emphasized that, to the best of our knowledge, this is the first and preliminary study aiming to evaluate the ocular tolerance of MPs loaded with the PEA and Citicoline. Actually, previous studies were mainly focused on the evaluation of GDNF loading in MPs, along with the technological characterization of the devices, and *in vitro* and *in vivo* assessment [20], [50], [85], [86].

Citicoline is an endogenous compound that acts as an intermediate in the synthesis of membrane phospholipids and specifically of phosphatidylcholine, which is a key component of cell membranes, and is involved in cell homeostasis conservation [87]. Based on this body of knowledge, Citicoline has been widely studied for its neuroprotective and neuro-enhancing role in neurological diseases such as stroke [88], brain injury, Alzheimer's and Parkinson's disease [89]. Nowadays, there is an increasing interest to investigate Citicoline for its possible role in ophthalmological diseases such as amblyopia [90] [91], optic neuropathies [87], glaucoma [92] and diabetic retinopathy [93]. Experimental *in vitro* and *in vivo* studies have shown that Citicoline has a neuroprotective effect on damaged RGCs since it is able to neutralize excitotoxicity due to glutamate action [93] [94] [95].

Palmitoylethanolamide (PEA) is an endogenous analogous of the endocannabinoid anandamide, which is endowed with a potent anti-inflammatory activity, that can be exploited in a wide array of pathological conditions and of biological systems, including retina [96] [97]. Many works have highlighted that PEA can play beneficial effects in several retinal diseases such as diabetic retinopathy, glaucoma, etc. In particular, it was found out that PEA can attenuate the degree of retinal inflammation while preserving the blood–retinal barrier in diabetic rats [98]. Moreover, systemic PEA treatment was found to be effective in optimizing visual field of glaucoma patients while decreasing intraocular pressure (IOP), which is the main risk factor of glaucoma [99]. Furthermore, topical ocular treatment with PEA was recently found to be effective in attenuating the inflammation of ocular surface in humans [100]. Despite the potential pharmacological applications of PEA, its clinical application is strongly compromised by an unfavorable pharmacokinetic profile, mainly due to its poor solubility in water. As a consequence, the topical application of PEA, for instance using

eye drops, is strongly constrained due to its unfavorable physico-chemical property. To overcome this limitation, the encapsulation of PEA in the MPs here produced was an attractive possibility, considering the amphiphilic nature of MP bulk that was expected to promote the apparent solubility of PEA, thereby enhancing, in principle, its ocular bioavailability.

The experiments indicate, for both PEA and Citicoline, the lack of toxicity *in vitro* after 4 days and, *in vivo*, after 7 days. In particular, the available data show that the encapsulation of both did not produce an apparent advantage compared to each free drug. This may seem discouraging at a first glance. However, long term studies, both technological and biological, are to be taken aiming to verify the actual biological performance of the drug and the feasibility of its microencapsulation. Also, the stability of these active molecules in the release times will be assessed.

These findings may have therapeutic relevance for glaucoma and other chronic diseases in which RPE degeneration is present and sustained amounts of active substances are required. Furthermore, different amounts of microparticles can be injected in the vitreous (that is, different doses) according to the patient's needs. Consequently, this therapeutic approach may be a useful long-term therapy as a more personalized strategy for chronic retinal pathologies such as AMD and glaucoma, where atrophy of the RPE develops and a degeneration of RGCs occurs, in contrast to intravitreal implants and eye drops, which are typically administered at fixed dose.

Chapter 6

CONCLUSIONS

Chapter 6

6. Conclusions

The results obtained in this study showed that the produced MPs are able to sustain the release of BSA for 4-6 weeks according to the formulation. This time frame is less than that hoped for, but it is nevertheless encouraging because it should be compared with the bolus administration of the active molecule. In principle, therefore, the produced devices are promising for the desired application and are also expected to provoke a lower intraocular concentration peak of the administered drug(s). Anyhow, formulation improvements will be necessary to further sustain the release of the loaded molecule(s).

Indeed, it is important to keep in mind is that the rate of protein release and device disappearance must match in optimized formulations. This is of extreme importance in the view of intravitreal administration, for which a strong requirement is the absence of MPs debris after each injection and, more importantly, in the long term. Thus, further work will be necessary to find out the actually "optimal" formulation, which ideally should leave no leftovers after the complete drug discharging.

Another issue to consider is that the injection procedure is quite complex as it involves the precise placement of the MP suspension in a blind area of the eye, close to the visual axis. The actual application in humans requires further studies to verify the feasibility of the administration as well as the righteousness of the hypothesis.

The *in vivo* results, although preliminary, are interesting since the safety profile of MPs has been confirmed in the times tested so far (7 days), in addition to the protective action against RCGs, which can be associated with the action of MPs or the trehalose. Specifically, the outcomes have demonstrated that MPs do not affect ARPE-19 cell viability and retina histology, therefore highlighting their safety of use.

Additional *in vivo* investigations are needed before carrying the fabricated MPs to the clinics since the actual biological effect of GNDF, PEA and Citicoline are unclear to date. A prolonged observation time will allow to shed light on the actual mechanisms underlying the observed effects to date. Such experiments are currently underway. Moreover, biodistribution and pharmacokinetic studies will be carried out, which will represent a fundamental basis for evaluating the real effectiveness of the produced MPs.

Taken together, the obtained results pave the way for manifold *in vivo* experimental campaigns to confirm the usefulness of the MPs produced. To reinforce the outcomes of this study, a further model of glaucoma will be chosen, in which the increase in intraocular pressure will be induced by the injection of microbeads. In detail, obstruction of the trabecular meshworh (TM) by the injection of microbeads will be carried out as a method for the generation of experimental glaucoma [101] [102] [103]. In the described glaucoma model, dysfunction and degeneration of RGC axons, which is a cardinal feature of the disease, will be also assessed.

In conclusion, the produced MPs hold promise as possible devices to be employed in the treatment of posterior eye segments, possibly other than glaucoma. However, further formulative studies are necessary to rationally effect the *in silico-in vivo* translation as well as the scale up to the industrial environment.

This is important to complete the investigation of this work since the use of intravitreal injections is expected to increase for the foreseeable future, mainly considering the worldwide ageing.

Chapter 7

BIBLIOGRAPHY

7. Bibliography

[1] H. E. D. M. Khalil, H. A. El Gendy, H. A. R. Youssef, H. E. Haroun, T. A. Gheita, and H. M. Bakir, "The Effectiveness of Intraocular Methotrexate in the Treatment of Posterior Uveitis in Behçet's Disease Patients Compared to Retrobulbar Steroids Injection," *J. Ophthalmol.*, vol. 2016, 2016, doi: 10.1155/2016/1678495.

[2] H. F. Edelhauser *et al.*, "Ophthalmic drug delivery systems for the treatment of retinal diseases: Basic research to clinical applications," *Investig. Ophthalmol. Vis. Sci.*, vol. 51, no. 11, pp. 5403–5420, 2010, doi: 10.1167/iovs.10-5392.

[3] D. H. Geroski and H. F. Edelhauser, "Transscleral drug delivery for posterior segment disease," *Adv. Drug Deliv. Rev.*, vol. 52, no. 1, pp. 37–48, 2001, doi: 10.1016/S0169-409X(01)00193-4.

[4] R. Herrero-Vanrell and M. F. Refojo, "Biodegradable microspheres for vitreoretinal drug delivery," *Adv. Drug Deliv. Rev.*, vol. 52, no. 1, pp. 5–16, 2001, doi: 10.1016/S0169-409X(01)00200-9.

[5] A. Balasopoulou *et al.*, "Symposium Recent advances and challenges in the management of retinoblastoma Globe - saving Treatments," *BMC Ophthalmol.*, vol. 17, no. 1, p. 1, 2017, doi: 10.4103/ijo.IJO.

[6] T. R. Thrimawithana, S. Young, C. R. Bunt, C. Green, and R. G. Alany, "Drug delivery to the posterior segment of the eye," *Drug Discov. Today*, vol. 16, no. 5–6, pp. 270–277, 2011, doi: 10.1016/j.drudis.2010.12.004.

[7] N. Bodor and P. Buchwald, "Ophthalmic drug design based on the metabolic activity of the eye: Soft drugs and chemical delivery systems," *AAPS J.*, vol. 7, no. 4, pp. 820–833, 2005, doi: 10.1208/aapsj070479.

[8] K. G. Falavarjani and Q. D. Nguyen, "Adverse events and complications associated with intravitreal injection of anti-VEGF agents: A review of literature," *Eye*, vol. 27, no. 7, pp. 787–794, 2013, doi: 10.1038/eye.2013.107.

[9] C. Martínez-Sancho, R. Herrero-Vanrell, and S. Negro, "Poly (D,L-lactide-co-glycolide) microspheres for long-term intravitreal delivery of aciclovir: Influence of fatty and non-fatty

additives," *J. Microencapsul.*, vol. 20, no. 6, pp. 799–810, 2003, doi: 10.1080/02652040310001600532.

[10] R. Gaudana, H. K. Ananthula, A. Parenky, and A. K. Mitra, "Ocular drug delivery.," *AAPS J.*, vol. 12, no. 3, pp. 348–360, 2010, doi: 10.1208/s12248-010-9183-3.

[11] K. M. Sampat and S. J. Garg, "Complications of intravitreal injections," *Curr. Opin. Ophthalmol.*, vol. 21, no. 3, pp. 178–183, 2010, doi: 10.1097/ICU.0b013e328338679a.

[12] T. Moritera, Y. Ogura, Y. Honda, R. Wada, S. H. Hyon, and Y. Ikada, "Microspheres of biodegradable polymers as a drug-delivery system in the vitreous.," *Invest. Ophthalmol. Vis. Sci.*, vol. 32, no. 6, pp. 1785–1790, 1991.

[13] A. Zimmer and J. Kreuter, "Microspheres and nanoparticles used in ocular delivery systems," *Adv. Drug Deliv. Rev.*, vol. 16, no. 1, pp. 61–73, 1995, doi: 10.1016/0169-409X(95)00017-2.

[14] J. A. Tamada and R. Langer, "Erosion kinetics of hydrolytically degradable polymers," *Proc. Natl. Acad. Sci. U. S. A.*, vol. 90, no. 2, pp. 552–556, 1993, doi: 10.1073/pnas.90.2.552.

[15] P. Checa-Casalengua *et al.*, "Retinal ganglion cells survival in a glaucoma model by GDNF/Vit e PLGA microspheres prepared according to a novel microencapsulation procedure," *J. Control. Release*, vol. 156, no. 1, pp. 92–100, 2011, doi: 10.1016/j.jconrel.2011.06.023.

[16] P. Adamson *et al.*, "Single ocular injection of a sustained-release anti-VEGF delivers 6 months pharmacokinetics and efficacy in a primate laser CNV model," *J. Control. Release*, vol. 244, pp. 1–13, 2016, doi: 10.1016/j.jconrel.2016.10.026.

[17] L. Mayol, M. Biondi, L. Russo, B. M. Malle, K. Schwach-Abdellaoui, and A. Borzacchiello, "Amphiphilic hyaluronic acid derivatives toward the design of micelles for the sustained delivery of hydrophobic drugs," *Carbohydr. Polym.*, vol. 102, no. 1, pp. 110–116, 2014, doi: 10.1016/j.carbpol.2013.11.003.

[18] C. Carnevale *et al.*, "Human vitreous concentrations of citicoline following topical application of citicoline 2% ophthalmic solution," *PLoS One*, vol. 14, no. 11, pp. 1–12, 2019, doi: 10.1371/journal.pone.0224982.

[19] C. Puglia *et al.*, "Innovative nanoparticles enhance N-palmitoylethanolamide intraocular delivery," *Front. Pharmacol.*, vol. 9, no. MAR, pp. 1–7, 2018, doi: 10.3389/fphar.2018.00285.

[20] C. García-Caballero *et al.*, “Photoreceptor preservation induced by intravitreal controlled delivery of gdnf and gdnf/melatonin in rhodopsin knockout mice,” *Mol. Vis.*, vol. 24, no. May 2017, pp. 733–745, 2018.

[21] G. Velez and S. M. Whitcup, “New developments in sustained release drug delivery for the treatment of intraocular disease,” *Br. J. Ophthalmol.*, vol. 83, no. 11, pp. 1225–1229, 1999, doi: 10.1136/bjo.83.11.1225.

[22] M. Almasieh and L. A. Levin, “Neuroprotection in Glaucoma: Animal Models and Clinical Trials,” *Annu. Rev. Vis. Sci.*, vol. 3, pp. 91–120, 2017, doi: 10.1146/annurev-vision-102016-061422.

[23] A. L. Pelletier, L. Rojas-Roldan, and J. Coffin, “Vision loss in older adults,” *Am. Fam. Physician*, vol. 94, no. 3, pp. 219–226, 2016.

[24] M. Almasieh, A. M. Wilson, B. Morquette, J. L. Cueva Vargas, and A. Di Polo, “The molecular basis of retinal ganglion cell death in glaucoma,” *Prog. Retin. Eye Res.*, vol. 31, no. 2, pp. 152–181, 2012, doi: 10.1016/j.preteyeres.2011.11.002.

[25] G. Peyman, D.W. Vastin, H.I. Meisels, The experimental and clinical use of intravitreal antibiotics to treat bacterial and fungal endophthalmitis. Documenta Ophthalmologica 39,1 : 183-201, 1975.

[26] A. Subrizi, E. M. del Amo, V. Korzhikov-Vlakh, T. Tennikova, M. Ruponen, and A. Urtti, “Design principles of ocular drug delivery systems: importance of drug payload, release rate, and material properties,” *Drug Discov. Today*, vol. 24, no. 8, pp. 1446–1457, 2019, doi: 10.1016/j.drudis.2019.02.001.

[27] E. M. Del Amo, K. S. Vellonen, H. Kidron, and A. Urtti, “Intravitreal clearance and volume of distribution of compounds in rabbits: In silico prediction and pharmacokinetic simulations for drug development,” *Eur. J. Pharm. Biopharm.*, vol. 95, pp. 215–226, 2015, doi: 10.1016/j.ejpb.2015.01.003.

[28] L. Pitkänen, V. P. Ranta, H. Moilanen, and A. Urtti, “Permeability of retinal pigment epithelium: Effects of permeant molecular weight and lipophilicity,” *Investig. Ophthalmol. Vis. Sci.*, vol. 46, no. 2, pp. 641–646, 2005, doi: 10.1167/iovs.04-1051.

[29] T. Yasukawa, Y. Ogura, Y. Tabata, H. Kimura, P. Wiedemann, and Y. Honda, “Drug delivery systems for vitreoretinal diseases,” *Prog. Retin. Eye Res.*, vol. 23, no. 3, pp. 253–281, 2004, doi: 10.1016/j.preteyeres.2004.02.003.

[30] R. Herrero-Vanrell, I. Bravo-Osuna, V. Andrés-Guerrero, M. Vicario-de-la-Torre, and I. T. Molina-Martínez, "The potential of using biodegradable microspheres in retinal diseases and other intraocular pathologies," *Prog. Retin. Eye Res.*, vol. 42, pp. 27–43, 2014, doi: 10.1016/j.preteyeres.2014.04.002.

[31] I. S. Ganciclovir *et al.*, "Intravitreal Sustained-Release Ganciclovir," 2015.

[32] G. J. Jaffe, C. H. Yang, H. Guo, J. P. Denny, C. Lima, and P. Ashton, "Fluocinolone Acetonide Sustained Delivery Device AND," *Invest. Ophthalmol.*, pp. 3569–3575, 1996.

[33] F. E. Kane and K. E. Green, "Ocular pharmacokinetics of fluocinolone acetonide following iluvien implantation in the vitreous humor of rabbits," *J. Ocul. Pharmacol. Ther.*, vol. 31, no. 1, pp. 11–16, 2015, doi: 10.1089/jop.2014.0100.

[34] A. Chan, L. S. Leung, and M. S. Blumenkranz, "Critical appraisal of the clinical utility of the dexamethasone intravitreal implant (Ozurdex®) for the treatment of macular edema related to branch retinal vein occlusion or central retinal vein occlusion," *Clin. Ophthalmol.*, vol. 5, no. 1, pp. 1043–1049, 2011, doi: 10.2147/OPTH.S13775.

[35] S. K. L. Seah *et al.*, "Use of surodex in phacotrabeculectomy surgery," *Am. J. Ophthalmol.*, vol. 139, no. 5, pp. 927–928, 2005, doi: 10.1016/j.ajo.2004.10.052.

[36] D. T. H. Tan, S. P. Chee, L. Lim, J. Theng, and M. Van Ede, "Randomized clinical trial of surodex steroid drug delivery system for cataract surgery: Anterior versus posterior placement of two surodex in the eye," *Ophthalmology*, vol. 108, no. 12, pp. 2172–2181, 2001, doi: 10.1016/S0161-6420(01)00839-9.

[37] R. Herrero-Vanrell, M. Vicario De La Torre, V. Andrés-Guerrero, D. Barbosa-Alfaro, I. T. Molina-Martínez, and I. Bravo-Osuna, "Nano and microtechnologies for ophthalmic administration, an overview," *J. Drug Deliv. Sci. Technol.*, vol. 23, no. 2, pp. 75–102, 2013, doi: 10.1016/S1773-2247(13)50016-5.

[38] R. A. Jain, "The manufacturing techniques of various drug loaded biodegradable poly(lactide-co-glycolide) (PLGA) devices," *Biomaterials*, vol. 21, no. 23, pp. 2475–2490, 2000, doi: 10.1016/S0142-9612(00)00115-0.

[39] H. Tamber, P. Johansen, H. P. Merkle, and B. Gander, "Formulation aspects of biodegradable polymeric microspheres for antigen delivery," *Adv. Drug Deliv. Rev.*, vol. 57, no. 3 SPEC. ISS., pp. 357–376, 2005, doi: 10.1016/j.addr.2004.09.002.

[40] F. Danhier, E. Ansorena, J. M. Silva, R. Coco, A. Le Breton, and V. Préat, "PLGA-based nanoparticles: An overview of biomedical applications," *J. Control. Release,* vol. 161, no. 2, pp. 505–522, 2012, doi: 10.1016/j.jconrel.2012.01.043.

[41] N. B. Shelke, R. Kadam, P. Tyagi, V. R. Rao, and U. B. Kompella, "Intravitreal poly(l-lactide) microparticles sustain retinal and choroidal delivery of TG-0054, a hydrophilic drug intended for neovascular diseases," *Drug Deliv. Transl. Res.*, vol. 1, no. 1, pp. 76–90, 2011, doi: 10.1007/s13346-010-0009-8.

[42] J. A. Schrier and P. P. DeLuca, "Porous bone morphogenetic protein-2 microspheres: Polymer binding and in vitro release," *AAPS PharmSciTech,* vol. 2, no. 3, 2001, doi: 10.1208/pt020317.

[43] S. Yang, K. F. Leong, Z. Du, and C. K. Chua, "The design of scaffolds for use in tissue engineering. Part I. Traditional factors," *Tissue Eng.,* vol. 7, no. 6, pp. 679–689, 2001, doi: 10.1089/107632701753337645.

[44] K. Park, "Tolerance levels of PLGA microspheres in the eyes," *J. Control. Release,* vol. 266, p. 365, 2017, doi: 10.1016/j.jconrel.2017.11.010.

[45] K. Y. Cho, S. H. Choi, C. H. Kim, Y. S. Nam, T. G. Park, and J. K. Park, "Protein release microparticles based on the blend of poly (D,L-lactic-co-glycolic acid) and oligo-ethylene glycol grafted poly(L-lactide)," *J. Control. Release*, vol. 76, no. 3, pp. 275–284, 2001, doi: 10.1016/S0168-3659(01)00442-4.

[46] M. L. Houchin and E. M. Topp, "Physical properties of PLGA films during polymer degradation," *J. Appl. Polym. Sci.*, vol. 114, no. 5, pp. 2848–2854, 2009, doi: 10.1002/app.30813.

[47] L. Lu *et al.*, "In vitro degradation of porous poly(L-lactic acid) foams," *Biomaterials,* vol. 21, no. 15, pp. 1595–1605, 2000, doi: 10.1016/S0142-9612(00)00048-X.

[48] C. Thomasin, H. Nam-Trân, H. P. Merkle, and B. Gander, "Drug microencapsulation by PLA/PLGA coacervation in the light of thermodynamics. 1. Overview and theoretical considerations," *J. Pharm. Sci.,* vol. 87, no. 3, pp. 259–268, 1998, doi: 10.1021/js970047r.

[49] Z. Ye, Y. L. Ji, X. Ma, J. G. Wen, W. Wei, and S. M. Huang, "Pharmacokinetics and distributions of bevacizumab by intravitreal injection of bevacizumab- PLGA microspheres in rabbits," *Int. J. Ophthalmol.*, vol. 8, no. 4, pp. 653–658, 2015, doi: 10.3980/j.issn.2222-3959.2015.04.02.

[50] C. García-Caballero *et al.*, "Six month delivery of GDNF from PLGA/vitamin E biodegradable microspheres after intravitreal injection in rabbits," *Eur. J. Pharm. Sci.*, vol. 103, pp. 19–26, 2017, doi: 10.1016/j.ejps.2017.02.037.

[51] J. Liu *et al.*, "Highly bioactive, bevacizumab-loaded, sustained-release PLGA/PCADK microspheres for intravitreal therapy in ocular diseases," *Int. J. Pharm.*, vol. 563, no. March, pp. 228–236, 2019, doi: 10.1016/j.ijpharm.2019.04.012.

[52] X. Mo *et al.*, "Effects of erythropoietin-dextran microparticle-based PLGA/PLA microspheres on RGCS," *Investig. Ophthalmol. Vis. Sci.*, vol. 53, no. 10, pp. 6025–6034, 2012, doi: 10.1167/iovs.12-9898.

[53] C. Harada *et al.*, "Potential role of glial cell line-derived neurotrophic factor receptors in Müller glial cells during light-induced retinal degeneration," *Neuroscience*, vol. 122, no. 1, pp. 229–235, 2003, doi: 10.1016/S0306-4522(03)00599-2.

[54] M. Zhao *et al.*, "Tolerance of high and low amounts of PLGA microspheres loaded with mineralocorticoid receptor antagonist in retinal target site," *J. Control. Release*, vol. 266, no. June, pp. 187–197, 2017, doi: 10.1016/j.jconrel.2017.09.029.

[55] L. Fernández-Sánchez *et al.*, "Controlled delivery of tauroursodeoxycholic acid from biodegradable microspheres slows retinal degeneration," *PLoS One*, vol. 12, no. 5, pp. 1–20, 2017, doi: 10.1371/journal.pone.0177998.

[56] J. Liu *et al.*, "Anti-angiogenic activity of bevacizumab-bearing dexamethasone-loaded PLGA nanoparticles for potential intravitreal applications," *Int. J. Nanomedicine*, vol. 14, pp. 8819–8834, 2019, doi: 10.2147/IJN.S217038.

[57] P. Bhatt, G. Fnu, D. Bhatia, A. Shahid, and V. Sutariya, "Nanodelivery of Resveratrol-Loaded PLGA Nanoparticles for Age-Related Macular Degeneration," *AAPS PharmSciTech*, vol. 21, no. 8, pp. 1–9, 2020, doi: 10.1208/s12249-020-01836-4.

[58] P. Narvekar, P. Bhatt, G. Fnu, and V. Sutariya, "Axitinib-Loaded Poly(Lactic-Co-Glycolic Acid) Nanoparticles for Age-Related Macular Degeneration: Formulation Development and in Vitro Characterization," *Assay Drug Dev. Technol.*, vol. 17, no. 4, pp. 167–177, 2019, doi: 10.1089/adt.2019.920.

[59] F. Qiu *et al.*, "Fenofibrate-Loaded Biodegradable Nanoparticles for the Treatment of Experimental Diabetic Retinopathy and Neovascular Age-Related Macular Degeneration,"

Mol. Pharm., vol. 16, no. 5, pp. 1958–1970, 2019, doi: 10.1021/acs.molpharmaceut.8b01319.

[60] B. Xie *et al.*, "An injectable thermosensitive polymeric hydrogel for sustained release of Avastin1 to treat posterior segment disease," *Int. J. Pharm.*, vol. 490, no. 1–2, pp. 375–383, 2015, doi: 10.1016/j.ijpharm.2015.05.071.

[61] C. C. Hu, J. R. Chaw, C. F. Chen, and H. W. Liu, "Controlled release bevacizumab in thermoresponsive hydrogel found to inhibit angiogenesis," *Biomed. Mater. Eng.*, vol. 24, no. 6, pp. 1941–1950, 2014, doi: 10.3233/BME-141003.

[62] C. R. Osswald and J. J. Kang-Mieler, "Controlled and Extended In Vitro Release of Bioactive Anti-Vascular Endothelial Growth Factors from a Microsphere-Hydrogel Drug Delivery System," *Curr. Eye Res.*, vol. 41, no. 9, pp. 1216–1222, 2016, doi: 10.3109/02713683.2015.1101140.

[63] T. C. Laurent and J. R. E. Fraser, " Hyaluronan 1 ," *FASEB J.*, vol. 6, no. 7, pp. 2397–2404, 1992, doi: 10.1096/fasebj.6.7.1563592.

[64] N. M. Salwowska, K. A. Bebenek, D. A. Żądło, and D. L. Wcisło-Dziadecka, "Physiochemical properties and application of hyaluronic acid: a systematic review," *J. Cosmet. Dermatol.*, vol. 15, no. 4, pp. 520–526, 2016, doi: 10.1111/jocd.12237.

[65] S. Giarra *et al.*, "Spontaneous arrangement of a tumor targeting hyaluronic acid shell on irinotecan loaded PLGA nanoparticles," *Carbohydr. Polym.*, vol. 140, pp. 400–407, 2016, doi: 10.1016/j.carbpol.2015.12.031.

[66] C. Serri *et al.*, "Combination therapy for the treatment of pancreatic cancer through hyaluronic acid-decorated nanoparticles loaded with quercetin and gemcitabine: A preliminary in vitro study," *J. Cell. Physiol.*, vol. 234, no. 4, pp. 4959–4969, 2019, doi: 10.1002/jcp.27297.

[67] M. P. Kummer, J. J. Abbott, S. Dinser, and B. J. Nelson, "Artificial vitreous humor for in vitro experiments.," *Conf. Proc. IEEE Eng. Med. Biol. Soc.*, pp. 6407–6410, 2007.

[68] O. I. Corrigan and X. Li, "Quantifying drug release from PLGA nanoparticulates," *Eur. J. Pharm. Sci.*, vol. 37, no. 3–4, pp. 477–485, 2009, doi: 10.1016/j.ejps.2009.04.004.

[69] R. P. Batycky, J. Hanes, R. Langer, and D. A. Edwards, "A theoretical model of erosion and macromolecular drug release from biodegrading microspheres," *J. Pharm. Sci.*, vol. 86, no. 12, pp. 1464–1477, 1997, doi: 10.1021/js9604117.

[70] S. Kuehn *et al.*, “The novel induction of retinal ganglion cell apoptosis in porcine organ culture by NMDA - An opportunity for the replacement of animals in experiments,” *ATLA Altern. to Lab. Anim.*, vol. 44, no. 6, pp. 557–568, 2016, doi: 10.1177/026119291604400608.

[71] Q. Xu *et al.*, “Nanoparticle diffusion in, and microrheology of, the bovine vitreous ex vivo,” *J. Control. Release*, vol. 167, no. 1, pp. 76–84, 2013, doi: 10.1016/j.jconrel.2013.01.018.

[72] N. K. Tram and K. E. Swindle-Reilly, “Rheological properties and age-related changes of the human vitreous humor,” *Front. Bioeng. Biotechnol.*, vol. 6, no. DEC, pp. 1–12, 2018, doi: 10.3389/fbioe.2018.00199.

[73] P. Blasi, S. S. D’Souza, F. Selmin, and P. P. DeLuca, “Plasticizing effect of water on poly(lactide-co-glycolide),” *J. Control. Release*, vol. 108, no. 1, pp. 1–9, 2005, doi: 10.1016/j.jconrel.2005.07.009.

[74] K. Dixit, R. B. Athawale, and S. Singh, “Quality control of residual solvent content in polymeric microparticles,” *J. Microencapsul.*, vol. 32, no. 2, pp. 107–122, 2015, doi: 10.3109/02652048.2014.995730.

[75] C. C. Camarasu, “Unknown residual solvents identification in drug products by headspace solid phase microextraction gas chromatography-mass spectrometry,” *Chromatographia*, vol. 56, no. SUPPL., 2002, doi: 10.1007/bf02494126.

[76] K. R. Dhangar, R. B. Jagtap, S. J. Surana, and A. A. Shirkhedkar, “Karakterizacija Na Nepoznati 4,” vol. 2, 2017.

[77] S. A. Aldossary, “Review on pharmacology of cisplatin: Clinical use, toxicity and mechanism of resistance of cisplatin,” *Biomed. Pharmacol. J.*, vol. 12, no. 1, pp. 7–15, 2019, doi: 10.13005/bpj/1608.

[78] P. Tsoka *et al.*, “intra,” *Exp. Eye Res.*, vol. 181, no. January, pp. 136–144, 2019, doi: 10.1016/j.exer.2019.01.018.

[79] C. Wang, H. Hou, K. Nan, M. J. Sailor, W. R. Freeman, and L. Cheng, “Intravitreal controlled release of dexamethasone from engineered microparticles of porous silicon dioxide,” *Exp. Eye Res.*, vol. 129, pp. 74–82, 2014, doi: 10.1016/j.exer.2014.11.002.

[80] Y. Fu, W. J. Kao, Drug Release Kinetics and Transport Mechanisms of Non-degradable and Degradable Polymeric Delivery Systems". Expert Opin Drug Deliv. 7(4): 429–444. 2010,

doi:10.1517/17425241003602259

[81] J. Siepmann and A. Göpferich, “Mathematical modeling of bioerodible, polymeric drug delivery systems,” *Adv. Drug Deliv. Rev.*, vol. 48, no. 2–3, 2001, doi: 10.1016/S0169-409X(01)00116-8.

[82] F. Von Burkersroda, L. Schedl, and A. Göpferich, “Why degradable polymers undergo surface erosion or bulk erosion,” *Biomaterials*, vol. 23, no. 21, 2002, doi: 10.1016/S0142-9612(02)00170-9.

[83] G. G. Giordano, P. Chevez-Barrios, M. F. Refojo, and C. A. Garcia, “Biodegradation and tissue reaction to intravitreous biodegradable poly(d,l-lactic-co-glycolic)acid microspheres,” *Curr. Eye Res.*, vol. 14, no. 9, pp. 761–768, 1995, doi: 10.3109/02713689508995797.

[84] J. A. Cardillo, A. A. Souza-Filho, and A. G. Oliveira, “Intravitreal Bioerudivel sustained-release triamcinolone microspheres system (RETAAC). Preliminary report of its potential usefulnes for the treatment of diabetic macular edema.,” *Arch. Soc. Esp. Oftalmol.*, vol. 81, no. 12, pp. 675–7, 679–81, 2006, [Online]. Available: http://www.ncbi.nlm.nih.gov/pubmed/17199160.

[85] A. Arranz-Romera *et al.*, “A safe gdnf and gdnf/bdnf controlled delivery system improves migration in human retinal pigment epithelial cells and survival in retinal ganglion cells: Potential usefulness in degenerative retinal pathologies,” *Pharmaceuticals*, vol. 14, no. 1, pp. 1–24, 2021, doi: 10.3390/ph14010050.

[86] A. Arranz-Romera, S. Esteban-Pérez, I. T. Molina-Martínez, I. Bravo-Osuna, and R. Herrero-Vanrell, “Co-delivery of glial cell–derived neurotrophic factor (GDNF) and tauroursodeoxycholic acid (TUDCA) from PLGA microspheres: potential combination therapy for retinal diseases,” *Drug Deliv. Transl. Res.*, vol. 11, no. 2, pp. 566–580, 2021, doi: 10.1007/s13346-021-00930-9.

[87] G. Roberti *et al.*, “Cytidine 51-diphosphocholine (Citicoline) in glaucoma: Rationale of its use, current evidence and future perspectives,” *Int. J. Mol. Sci.*, vol. 16, no. 12, pp. 28401–28417, 2015, doi: 10.3390/ijms161226099.

[88] J. J. Secades *et al.*, “Citicoline for Acute Ischemic Stroke: A Systematic Review and Formal Meta-analysis of Randomized, Double-Blind, and Placebo-Controlled Trials,” *J. Stroke Cerebrovasc. Dis.*, vol. 25, no. 8, pp. 1984–1996, 2016, doi: 10.1016/j.jstrokecerebrovasdis.2016.04.010.

[89] P. Gareri *et al.*, "The Citicholinage Study: Citicoline Plus Cholinesterase Inhibitors in Aged Patients Affected with Alzheimer's Disease Study," *J. Alzheimer's Dis.*, vol. 56, no. 2, pp. 557–565, 2017, doi: 10.3233/JAD-160808.

[90] V. Porciatti, C. Schiavi, P. Benedetti, A. Baldi, and E. C. Campos, "Cytidine-5'-diphosphocholine improves visual acuity, contrast sensitivity and visually-evoked potentials of amblyopic subjects," *Curr. Eye Res.*, vol. 17, no. 2, pp. 141–148, 1998, doi: 10.1076/ceyr.17.2.141.5606.

[91] M. Fresina, A. Dickmann, A. Salerni, F. De Gregorio, and E. C. Campos, "Effect of oral CDP-choline on visual function in young amblyopic patients," *Graefe's Arch. Clin. Exp. Ophthalmol.*, vol. 246, no. 1, pp. 143–150, 2008, doi: 10.1007/s00417-007-0621-6.

[92] V. Parisi, G. Manni, G. Colacino, and M. G. Bucci, "Improves Retinal and Cortical Responses in," no. May, pp. 1126–1134, 1998.

[93] P. Bogdanov *et al.*, "Effects of liposomal formulation of citicoline in experimental diabetes-induced retinal neurodegeneration," *Int. J. Mol. Sci.*, vol. 19, no. 8, 2018, doi: 10.3390/ijms19082458.

[94] H. P. Chang *et al.*, "Neuroprotective effect of citicoline against KA-induced neurotoxicity in the rat retina," *Exp. Eye Res.*, vol. 81, no. 3, pp. 350–358, 2005, doi: 10.1016/j.exer.2005.02.007.

[95] A. Matteucci *et al.*, "Neuroprotective effects of citicoline in in vitro models of retinal neurodegeneration," *Int. J. Mol. Sci.*, vol. 15, no. 4, pp. 6286–6297, 2014, doi: 10.3390/ijms15046286.

[96] I. Matias, J. W. Wang, A. S. Moriello, A. Nieves, D. F. Woodward, and V. Di Marzo, "Changes in endocannabinoid and palmitoylethanolamide levels in eye tissues of patients with diabetic retinopathy and age-related macular degeneration," *Prostaglandins Leukot. Essent. Fat. Acids*, vol. 75, no. 6, pp. 413–418, 2006, doi: 10.1016/j.plefa.2006.08.002.

[97] S. Petrosino, T. Iuvone, and V. Di Marzo, "N-palmitoyl-ethanolamine: Biochemistry and new therapeutic opportunities," *Biochimie*, vol. 92, no. 6, pp. 724–727, 2010, doi: 10.1016/j.biochi.2010.01.006.

[98] I. Paterniti *et al.*, "Palmitoylethanolamide treatment reduces retinal inflammation in streptozotocin-induced diabetic rats," *Eur. J. Pharmacol.*, vol. 769, pp. 313–323, 2015, doi: 10.1016/j.ejphar.2015.11.035.

[99] C. Gagliano *et al.*, "Ocular hypotensive effect of oral palmitoyl-ethanolamide: A clinical trial," *Investig. Ophthalmol. Vis. Sci.*, vol. 52, no. 9, pp. 6096–6100, 2011, doi: 10.1167/iovs.10-7057.

[100] A. Di Zazzo, G. Roberti, A. Mashaghi, T. B. Abud, D. Pavese, and S. Bonini, "Use of Topical Cannabinomimetic Palmitoylethanolamide in Ocular Surface Disease Associated with Antiglaucoma Medications," *J. Ocul. Pharmacol. Ther.*, vol. 33, no. 9, pp. 670–677, 2017, doi: 10.1089/jop.2016.0117.

[101] W. Huang *et al.*, "Comparative analysis of retinal ganglion cell damage in three glaucomatous rat models," *Exp. Eye Res.*, vol. 172, no. March, pp. 112–122, 2018, doi: 10.1016/j.exer.2018.03.019.

[102] Y. A. Ito, N. Belforte, J. L. Cueva Vargas, and A. di Polo, "A magnetic microbead occlusion model to induce ocular hypertension-dependent glaucoma in mice," *J. Vis. Exp.*, vol. 2016, no. 109, pp. 1–10, 2016, doi: 10.3791/53731.

[103] J. E. Morgan and J. R. Tribble, "Microbead models in glaucoma," *Exp. Eye Res.*, vol. 141, pp. 9–14, 2015, doi: 10.1016/j.exer.2015.06.020.

LIST OF PUBLICATIONS:

- Hyaluronan-coated nanoparticles for active tumor targeting: Influence of polysaccharide molecular weight on cell uptake Francesca Della Sala(°) , Teresa Silvestri(°), Assunta Borzacchiello, Laura Mayol, Luigi Ambrosio, Marco Biondi. Colloids and Surfaces B: Biointerfaces. 2022, 210, 112240. doi.org/10.1016/j.colsurfb.2021.112240. (°):equal contribution.

- How poloxamer addition in hyaluronic-acid-decorated biodegradable microparticles affects polymer degradation and protein release kinetics. Teresa Silvestri, Barbara Immirzi, Giovanni Dal Poggetto, Paola Di Donato, Valentina Mollo, Laura Mayol, Marco Biondi. Applied Sciences. 2021, 11, 7567. doi.org/10.3390/app11167567

- Phase solubility and thermoanalytical studies of the inclusion complex formation between curcumin and hydroxypropyl-β-cyclodextrin in hydroalcoholic solutions. Dhovidon Kabirov(°), Teresa Silvestri(°), Marcella Niccoli, Laura Mayol, Marco Biondi, Concetta Giancola. 2020. Journal of Thermal Analysis and Calorimetry. doi.org/10.1007/s10973-020-10381-y. (°):equal contribution.

- Cell internalization kinetics of biodegradable nanoparticles decorated with hyaluronic acid. Teresa Silvestri, Laura Mayol, Assunta Borzacchiello, Francesca della Sala, Marco Biondi. (2020). Pharmaceutics, 12(4), 350; doi.org/10.3390/pharmaceutics12040350

- Skin permeation and thermodynamic features of curcumin-loaded liposomes. Virginia Campani, Lorena Scotti, Teresa Silvestri, Marco Biondi, Giuseppe De Rosa. (2020) Journal of Materials Science: Materials in Medicine. 31:18. doi.org/10.1007/s10856-019-6351-6

- Drug micro-carriers with a hyaluronic acid corona toward a diffusion limited aggregation within the vitreous body. Laura Mayol, Teresa Silvestri, Sabato Fusco, Assunta Borzacchiello, Giuseppe De Rosa, Marco Biondi. (2019) Carbohydrate Polymers, 220, 185–190. doi.org/10.1016/j.carbpol.2019.05.065

WORKSHOPS

POSTER PRESENTATION:

- "Drug micro-carriers with a hyaluronic acid corona toward a diffusion-limited aggregation within the vitreous body". Teresa Silvestri Laura Mayol, Assunta Borzacchiello, Giuseppe De Rosa, Marco Biondi. 13th A.it.U.N. "New Challenges in Self-assembling drug delivery Systems". June 13th -14th 2019 - Borgo Lanciano Relais, Castelraimondo, MC (Italy). Poster presentation.

- "Chemical reaction-free coating of biodegradable nanoparticles with hyaluronic acid. Cell uptake experiments and mathematical modelling." Marco Biondi, Assunta Borzacchiello, Francesca della Sala, Teresa Silvestri, Laura Mayol. 3rd European Conference on Pharmaceutics. 26th-27th March 2019. Bologna, Italy. Poster presentation.

- "Cell internalization kinetics of biodegradable nanoparticles decorated with hyaluronic acid". Teresa Silvestri, Laura Mayol, Assunta Borzacchiello, Francesca della Sala, Marco Biondi. 12° Convegno della Divisione di Tecnologia Farmaceutica – SCI. Pharmaceutical Technology, is a contamination of knowledge possible?". 12th-13th September 2019 – San Domenico Hotel, Soverato, CZ (Italy). Poster presentation.

- "Spectroscopic and thermoanalytic studies on the complex formation between curcumin and hydroxypropyl-b-cyclodextrin." Teresa Silvestri, Marco Biondi, Marcella Niccoli, Dhovidon Kabirov, Laura Mayol, Concetta Giancola. Central and Eastern European and 14th Mediterranean Joint Consortium on Calorimetry and Thermal Analysis. 27th-30th August 2019. Rome, Italy. Poster presentation.

- "Cell internalization kinetics of biodegradable nanoparticles decorated with hyaluronic acid". Teresa Silvestri, Laura Mayol, Assunta Borzacchiello, Francesca della Sala, Marco Biondi. CRS Italy Chapter. 7th-9th November 2019 – Catania (Italy). Poster presentation.

- MITO – un viaggio tra nanomedicina e direzionamento di farmaci. 13th-14th February 2020 Milan-Turin (Italy).

- "Phase solubility and thermoanalytical studies of the inclusion complex formation between curcumin and hydroxypropyl-β-cyclodextrin in hydroalcoholic solutions". Teresa Silvestri, Marco Biondi, Marcella Niccoli, Dhovidon Kabirov, Laura Mayol, Concetta Giancola. Chemistry and Technology of Functional Materials 7th-10thOctober 2020. Ivanovo, Russia. Poster presentation.

- "Biodegrable microparticles for the sustained intravitreal release of drugs in the treatment of posterior eye segment diseases". Teresa Silvestri Laura Mayol, Assunta Borzacchiello, Giuseppe De Rosa, Marco Biondi. CRS Virtual Annual Meeting – 29th June-2nd July 2020. Poster presentation.

- "Molecular weight influence of superficially exposed hyaluronic acid on nanoparticles cell internalization kinetics". Teresa Silvestri, Laura Mayol, Assunta Borzacchiello, Francesca della Sala, Marco Biondi. Young NanoInnavation. 17th-18thSeptember 2020. La Sapienza, Rome. (Italy). Poster presentation.

- "Drug micro-carriers with a hyaluronic acid corona toward a diffusion-limited aggregation within the vitreous body". Teresa Silvestri, Laura Mayol, Sabato Fusco, Assunta Borzacchiello, Giuseppe De Rosa, Marco Biondi. 12th World Meeting on Pharmaceutics, Biopharmaceutics and Pharmaceutical Technology. 11th-14th May 2021. Poster presentation.

- "Design and development of amphiphilic microparticles based on PLGA and decorated with hyaluronic acid". Teresa Silvestri, Laura Mayol, Sabato Fusco, Assunta Borzacchiello, Giuseppe De Rosa, Marco Biondi. CRS Virtual Annual Meeting – 25th-29th July 2021. Poster presentation.

ORAL PRESENTATION:

- Nuove sinergie tra Università ed Industria Farmaceutica". 25th October 2019 – Department of Pharmacy, University of Naples Federico II, Naples (Italy). Oral presentation.

- "Molecular weight influence of superficially exposed hyaluronic acid on nanoparticles cell internalization kinetics" Teresa Silvestri, Laura Mayol, Assunta Borzacchiello, Francesca della Sala, Marco Biondi. NanoInnovation. 15th-18th September 2020. La Sapienza, Roma. (Italy). Oral presentation.

- Controlled protein release from poly(lactic-co-glycolic acid) (PLGA)-based microparticles for intravitreal administration. Teresa Silvestri, Laura Mayol, Sabato Fusco, Assunta Borzacchiello, Giuseppe De Rosa, Marco Biondi. AMYC Biomed 2020. 13th-14th October 2020. Department of Pharmacy, University of Naples Federico II, Naples (Italy). Oral presentation.

- "Biodegradable microparticles for the treatment of the posterior eye segment diseases". Teresa Silvestri, Laura Mayol, Sabato Fusco, Assunta Borzacchiello, Giuseppe De Rosa, Marco Biondi. SCI 2021 – XXVII Congresso nazionale della società chimica italiana. 14th-23rd September 2021. Oral presentation.

SCHOOL ATTENDANCE:

- Spring School in Transferable skills. 13th-14th May 2019. Department of Pharmacy, Naples (Italy).

- "Cell internalization kinetics of biodegradable nanoparticles decorated with hyaluronic acid". Silvestri Teresa, Biondi Marco, Borzacchiello Assunta, della Sala Francesca, Mayol Laura. 19th Advanced School in Pharmaceutical Technology "Characterization of colloidal nanocarriers". 9th-12th September 2019 – Hotel San Domenico, CZ (Italy).

MEMBERSHIP:

- ADRITELF (Associazione Docenti e Ricercatori Italiani di Tecnologie e Legislazione Farmaceutiche)

- SCI (Società Chimica Italiana) - Divisione Tecnologia Farmaceutica

- CRS (Controlled Release Society)

- CRS Italy Chapter (Controlled Release Society)